

Durham E-Theses

Investigating the Mechanisms of Mutant-p53-Dependent Cell Engulfment in Cancer

PATTERSON, MARY, ISOBEL

How to cite:

PATTERSON, MARY, ISOBEL (2025) Investigating the Mechanisms of Mutant-p53-Dependent Cell Engulfment in Cancer, Durham theses, Durham University. Available at Durham E-Theses Online: http://etheses.dur.ac.uk/16303/

Use policy

The full-text may be used and/or reproduced, and given to third parties in any format or medium, without prior permission or charge, for personal research or study, educational, or not-for-profit purposes provided that:

- a full bibliographic reference is made to the original source
- a link is made to the metadata record in Durham E-Theses
- the full-text is not changed in any way

The full-text must not be sold in any format or medium without the formal permission of the copyright holders.

Please consult the full Durham E-Theses policy for further details.



Investigating the Mechanisms of Mutant-p53-Dependent Cell Engulfment in Cancer

Mary Isobel Patterson (Z0177024)

Department of Biosciences

Durham University

Supervisor: Dr Patricia Muller

Thesis submitted for the degree of Masters by Research (MRes)

Abstract

Cell-in-cell (CIC) structures form when one cell becomes internalised within another. While this can occur in homeostasis, it is most prevalent in cancer, and is commonly associated with aggressive tumour types and poor patient prognoses. Two contrasting models explain the mechanisms of cancer CIC formation: cannibalism, a phagocytic-like process driven by the outer cell, and entosis, in which the internal cell actively invades into its host. However, distinction between these two models is often unclear in the literature, and the underlying molecular mechanisms are poorly defined.

Our lab previously demonstrated that gain-of-function (GOF) mutations in the tumour suppressor, p53, promote CIC formation in cancer, with mutant p53 (mutp53) cells frequently assuming host cell fate. Based on live imaging, RhoA expression patterns, and FLIM analysis of membrane tension, we propose that mutp53-dependent engulfment is cannibalistic rather than entotic. We also demonstrate the role of SH3BGRL, a target gene of mutp53, in driving CIC formation and contributing to mutp53's GOF activity through anchorage-independent growth. Finally, immunofluorescence staining for SOX2 and ALDH1A1 indicates a possible association between CIC formation and cancer stemness. Together, these findings contribute to our understanding of the mechanisms of mutp53-dependent engulfment, and its potential impacts on worsening tumour progression.

Declaration

I declare that the contents of this work are original, and the work conducted is my own work, except where specific reference is made in the text to the work of others. This work has not been submitted in whole or in part for any other degree or qualification, except as specified.

Statement of Copyright

The copyright of this thesis rests with the author. No quotation from it should be published without the author's prior written consent and information derived from it should be acknowledged.

This thesis includes supplementary material from a co-authored publication:

Dolma, L., Patterson, M. I., Banyard, A., Hall, C., Bell, S., Breitwieser, W., Sahoo, S., Weightman, J., Gil, M. P., Ashton, G., Behan, C., Fullard, N., Williams, L. D. and Muller, P. A. (2025) 'Mutant p53 induces SH3BGRL expression to promote cell engulfment.' *Cell Death Discovery*, 11(1) 288.

Acknowledgements

Firstly, I would like to thank my supervisor Patricia Muller, who has been invaluable in guiding me through my project and supporting my development as a scientist. I am also very grateful to my fellow lab members, Steven, Hannah and Matt for all their advice and encouragement.

Tim, Joanne and Lydia in Bioimaging have been very patient with my many microscope-related questions, and Nicola and Lewis have been a great help with tissue culture. I am also grateful to Margarita Staykova for her support with FLIM experiments.

Finally, I would like to thank my family and friends for all their encouragement this past year. I am especially thankful to my parents who have supported me at every stage.

Contents

List of Abbreviations	7
List of Tables	9
List of Figures	9
Chapter 1: Introduction	10
1.1. p53 protein	10
1.2. Cell engulfment	12
1.3. Mutp53-dependent cell engulfment	16
1.4. SH3BGRL protein	18
1.5. Cancer stemness	19
1.6. Hypotheses and project aims	21
Chapter 2: Materials and Methods	22
2.1. Cell culture	22
2.2. Transient gene overexpression and knockdown	23
2.3. Confocal microscopy	23
2.4. Western blot analysis	27
2.5. Quantitative reverse transcription polymerase chain reaction (qRT-PCR)	28
2.6. Soft agar colony formation assay	29
2.7. Statistical analysis	30
Chapter 3: Characterisation of mutant-p53-dependent cell engulfment	31
3.1. Introduction and aims	31
3.2. Results	31
3.2.1. Validation of A431s as a model system for studying CIC formation	31
3.2.2. Optimising conditions for observing mutp53-dependent CIC formation in vitro	33
3.2.3. Mutp53-driven engulfment is reminiscent of cannibalism rather than entosis	35
3.2.4. Differences in plasma membrane tension are apparent within CIC structures	37
3.3. Discussion	40
Chapter 4: The role of SH3BGRL in mutant p53-dependent cell engulfment	42
4.1. Introduction and aims	42
4.2. Results	42
4.2.1. Loss or overexpression of SH3BGRL affects the frequency of CIC formation	42

4.2.2. SH3BGRL expression promotes anchorage-independent growth	45
4.3. Discussion	47
Chapter 5: CIC formation is associated with expression of cancer stemness markers	48
5.1. Introduction and aims	48
5.2. Results	48
5.2.1. Mutp53 cells express cancer stemness markers	48
5.2.2. Engulfing cells express cancer stemness markers	50
5.3. Discussion	52
Chapter 6: Conclusions and future directions	53
6.1. Key conclusions	53
6.2. Future directions	53
6.3. Wider significance	54
Bibliography	55

List of Abbreviations

ALDH1A1 aldehyde dehydrogenase 1 family member A1

BSA bovine serum albumin

CIC cell-in-cell

CSC cancer stem cell

CLSM confocal laser-scanning microscope

DAPI 4',6-diamidino-2-phenylindole

DMEM Dulbecco's modified eagle medium

DMSO dimethyl sulfoxide

DNA deoxyribonucleic acid

ECM extracellular matrix

EGFR epidermal growth factor receptor

EMT epithelial-to-mesenchymal transition

FACS fluorescence-activated cell sorting

FBS foetal bovine serum

FLIM fluorescence lifetime imaging microscopy

GAPDH glyceraldehyde 3-phosphate dehydrogenase

GFP green fluorescent protein

GOF gain-of-function

HER2 human epidermal growth factor receptor 2

KO knockout

KRAS Kirsten rat sarcoma virus MDM2 mouse double minute 2

MEF mouse embryonic fibroblast

MOPS 3-(N-morpholino) propane sulfonic acid

PBS phosphate-buffered saline PCR polymerase chain reaction

PDAC pancreatic ductal adenocarcinoma

PFA paraformaldehyde

poly(HEMA) poly(2-hydroxyethyl methacrylate)

RCP Rab-coupling protein
ROI region of interest
RNA ribonucleic acid

RT-qPCR reverse transcriptase quantitative polymerase chain reaction

SD standard deviation

SDS sodium dodecyl-sulphate

SDS-PAGE sodium dodecyl-sulphate polyacrylamide gel electrophoresis

SE standard error of the mean

SH3BGRL Src homology 3 domain binding glutamate rich protein like

siRNA small interference RNA

SOX2 SRY-box transcription factor 2

TEMED N,N,N',N'-tetramethylethylenediamine

TGF transforming growth factor

TIGAR TP53-induced glycolysis and apoptosis regulator

WT wild type

List of Tables

Table 1: Antibodies used for immunofluorescence staining	
Table 2: Antibodies used for immunoblotting	
Table 3: Primers used for qRT-PCR. 29	
List of Figures	
Figure 1: Mechanisms of cell-in-cell (CIC) formation in cancer	
Figure 2: Three criteria for the identification of CIC structures in fixed confocal imaging25	
Figure 3: Thresholding nuclei for counting in Fiji (ImageJ)	
Figure 4: Validation of A431s as a model system for studying CIC formation	
Figure 5: Determining the optimum time frame for observing cell engulfment	
Figure 6: CIC formation can be observed in fixed suspension cultures	
Figure 7: Live time-series imaging of mutant-p53-driven cell engulfment	
Figure 8: RhoA expression in mutp53 versus p53 KO cells	
Figure 9.1: Membrane tension in mutp53 versus p53 KO A431 cells	
Figure 9.2: Differences in membrane tension between engulfing and internal cells	
Figure 10.1: Transient SH3BGRL knockdown in control cells reduces mutp53-driven CIC	
formation	
Figure 10.2: Stable SH3BGRL overexpression in control cells promotes mutp53-driven CIC	
formation44	
Figure 11: Transient knockdown of SH3BGRL in mutp53 cells significantly reduces soft agar	
colony formation46	
Figure 12: Expression of cancer stemness markers in mutp53 versus p53 KO cells	
Figure 13: SOX2 expression is concentrated in CIC structures	
Figure 14: Engulfing cells express ALDH1A1	

Chapter 1: Introduction

1.1. p53 protein

1.1.1. p53 as the "guardian of the genome"

p53 is a transcription factor encoded by the *TP53* gene. Under physiological conditions, it functions as a tumour suppressor and master regulator of genomic integrity, coordinating cell cycle arrest, DNA repair, senescence, and apoptosis in response to stress. These multifaceted roles have earned p53 the title "guardian of the genome" (Feroz and Sheikh, 2020).

p53 is negatively regulated by the E3 ubiquitin ligase mouse double minute 2 (MDM2) through an autoregulatory feedback loop. Under normal conditions, p53 transcriptionally activates MDM2, which in turn binds to p53, ubiquitinates it, and targets it for degradation by the proteosome. This maintains low levels of p53 in healthy cells. However, in response to cellular stress (such as DNA damage, oncogene activation, or hypoxia) MDM2 is inhibited. This leads to p53 stabilisation and accumulation, enabling transcriptional activation of target genes involved in cell cycle arrest, DNA repair, and apoptosis (Moll and Petrenko, 2003).

1.1.2. p53 structure

The p53 protein comprises 393 amino acids organised into five functional domains: an N-terminal transactivation domain (the primary binding site for MDM2), a proline-rich region, a central DNA-binding domain, an oligomerisation domain, and a C-terminal regulatory domain. The oligomerisation domain regulates the assembly of p53 monomers into the active, tetrameric form of p53. The DNA-binding domain is the most frequent site of mutations; although alterations can occur at any of the 393 residues, there are six key hotspots within this region: R175, G245, R248, R249, R273, and R282 (Muller and Vousden, 2013). The presence of just one mutated p53 polypeptide can affect the function of the whole tetramer.

1.1.3. p53 mutations in cancer

Cancer arises through progressive accumulation of mutations that disrupt cellular homeostasis, leading to uncontrolled proliferation, evasion of cell death, and genomic instability. Given p53's central role in regulating genomic integrity, it is unsurprising that its dysfunction is closely associated with cancer development. In fact, p53 is the most frequently mutated protein in cancer, with at least 50% of all cancers harbouring p53 mutations (Soussi and Wiman, 2015).

While the majority of p53 mutations result in loss of protein function, mutant-p53 (mutp53) proteins can acquire additional functions that are not present in the wild-type. These can have multiple oncogenic effects, including increased survival, proliferation, metastasis, angiogenesis, chemoresistance, and genomic instability (Muller and Vousden, 2013). In support of this, mice engineered with 'gain-of-function' (GOF) p53 mutations develop lymphomas, sarcomas, and carcinomas which progress to metastasis. On the other hand, p53 knockout (KO) mice show only lymphomas and occasional sarcomas which are not particularly aggressive (Lang et al., 2004; Olive et al., 2004). It therefore stands to reason that mutp53 expression has been associated with earlier onset of cancer, more aggressive tumours, and poorer prognoses in patients (Yue et al., 2017).

1.1.4. Mutant p53 gain-of-function activity in cancer

There are numerous molecular mechanisms through which mutp53 promotes tumorigenesis. For example, mutp53 drives invasion by promoting the recycling of epidermal growth factor receptor (EGFR) and integrins via Rab-coupling protein (RCP). This allows for enhanced signalling, for example, from EGF to the kinase AKT which promotes invasiveness (Muller et al., 2009). Furthermore, mutp53 promotes tumour progression by inhibiting the interaction of Rac1 (a small GTPase) with SENP1; this favours the active form of Rac1, which contributes to metastasis (Yue et al., 2017). Mutp53 can also bind to and regulate the expression of transcription factors implicated in tumorigenesis, including HIF-1 α and NF-kB, as well as the p53 family members p63 and p73, to further enhance its GOF (Alvarado-Ortiz et al., 2021). Overall, while the full impact of mutp53 in cancer has not yet been elucidated, its expression is undoubtedly a significant driver of tumour progression.

1.2. Cell engulfment

1.2.1. Introduction to CIC formation

Cell engulfment is the process by which one cell becomes internalised within another, forming a 'cell-in-cell' (CIC) structure. Typically, the engulfing or external cell displays a crescent-shaped nucleus, while the internalised cell is enclosed within a vacuole. Despite having first been observed in tumour histology over 150 years ago (Eberth, 1864), relatively little is known about the mechanisms of CIC formation or the effects of engulfment on cancer development. In recent decades, however, advancements in imaging techniques have meant that this process can be examined in detail.

CIC structures have been observed in a wide range of human cancers, including melanoma (Lugini et al., 2006), breast cancer (S. Wang et al., 2016), lung adenocarcinoma (Mackay et al., 2018), pancreatic cancer (Cano et al., 2012), and colorectal cancer (Bozkurt et al., 2021). They are often found in the most aggressive tumours and are associated with enhanced levels of metastasis and drug resistance (Mackay and Muller, 2019). However, there is also evidence of a role for CIC structures in healthy tissue. For example, CIC formation has been observed during formation of cardiomyocytes (Belostotskaya et al., 2018), and blastocysts have been shown to engulf luminal epithelial cells during embryo implantation (Li et al., 2015).

CIC structures can be either homotypic, consisting of two or more cells from the same origin (for example, two tumour cells), or heterotypic, consisting of cells from different origins (for example, an immune cell inside a tumour cell) (Overholtzer and Brugge, 2008). There are numerous terms defining the types of CIC formation, including phagocytosis, in which cells engulf dead or apoptotic cells; enclysis, where a hepatocyte engulfs a T-lymphocyte; and emperipolesis, where an immune cell invades into a host which is also actively engulfing it. However, in the context of cancer, the two most prominent models are cannibalism, where a tumour cell extends protrusions allowing it to engulf another cell; and entosis, where a weaker tumour cell invades into a stronger one (Fais and Overholtzer, 2018).

1.2.2. Mechanisms of cell engulfment in cancer

Two main hypotheses, cannibalism and entosis, explain the formation of CIC structures in cancer (Figure 1). Cannibalism is driven by the external cell, which forms protrusions to encapsulate and internalise the other cell. On the other hand, entosis is driven by the internal cell; this is most often a weaker cancer cell which actively invades into a stronger one (Sun et al., 2014). However, understanding the nuances of these processes can prove difficult as much of the literature does not distinguish between them, focusing only on the resulting CIC structures.

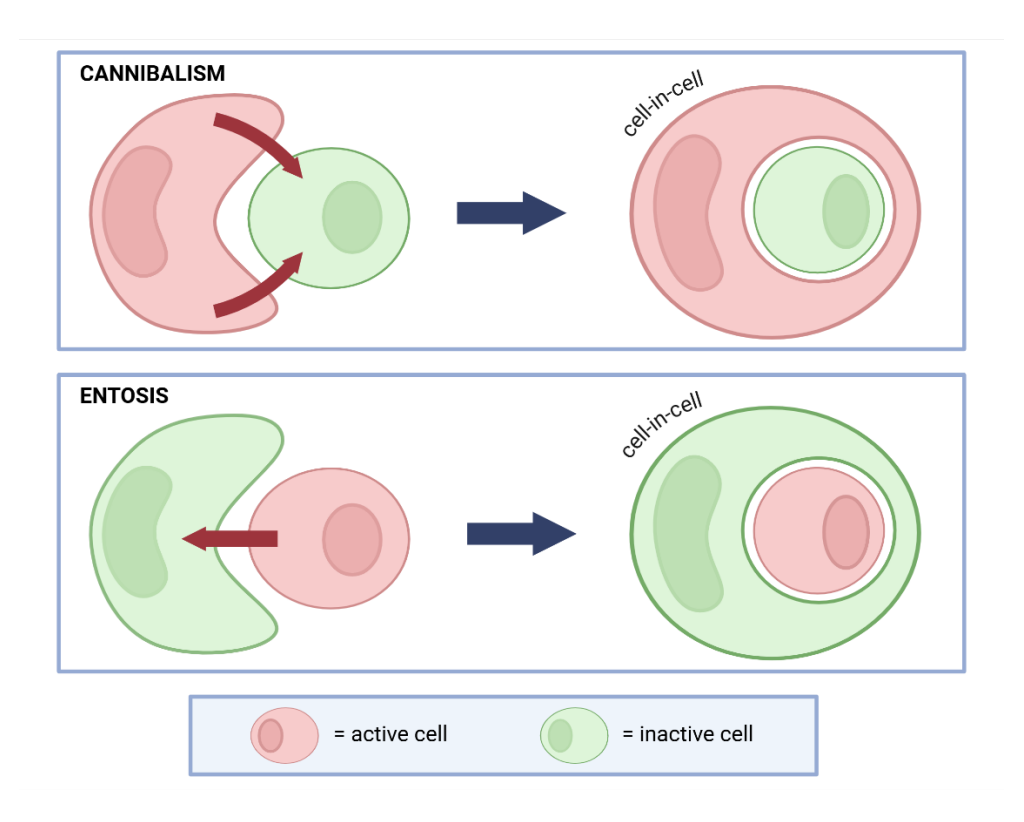


Figure 1: Mechanisms of cell-in-cell (CIC) formation in cancer.

In cannibalism, the host cell actively extends protrusions to wrap around and internalise its neighbour, forming a CIC structure. On the other hand, entosis is driven by the internal cell, which actively invades into the host.

Made with BioRender.com.

1.2.3. Molecular mechanisms of entosis

Overholtzer et al., (2007) first described entosis, hypothesising that this process depends on loss of cell attachment to the extracellular matrix (ECM). Normally, the compaction forces of Adherens junctions between cells are counterbalanced by binding of integrins to the ECM. However, in the absence of integrin-ECM engagement, differences in RhoA/ROCK-dependent contractile forces between the two cells result in one cell invading into the other; the other cell is then wrapped around.

During entotic engulfment, the two cells are thought to interact through epithelial cadherin-mediated cell-cell contacts. Evidencing this, Sun et al., (2014) showed that exogenous expression of E- or P-cadherin is sufficient to induce entosis in human breast cancer cells lacking these adhesion proteins. Mechanistically, the authors proposed that p190A RhoGAP is recruited to the junction between the host and entosing cell, leading to inhibition of RhoA in this region. The cell being internalised therefore has comparatively higher Rho activity in the region away from the adhesion; this allows the inner cell to actively push into its neighbour, forming a CIC structure.

Entosis has been described as a form of cell competition between tumour cells, with 'winner' cells engulfing and killing 'loser' cells. Interestingly, Sun et al. reported that expression of the oncogene KRAS can induce winner cell status by activating Rac1; this results in inhibition of actomyosin-mediated contractility. The winner cell therefore has greater mechanical deformability, so can mould itself around the more rigid loser cell. Overall, this represents a possible mechanism by which 'fitter,' oncogene-expressing cells could outcompete wild-type cells in heterogenous tumour populations. This is significant in terms of tumour initiation as destruction of wild-type cells in this way could allow oncogene-expressing cells to invade into healthy tissue (Sun et al., 2015).

1.2.4. Molecular mechanisms of cannibalism

Comparatively little is known about the molecular pathways driving cannibalism. However, there are mechanistic parallels between cannibalism and phagocytosis, notably the extension of protrusions to wrap around and engulf the internal cell. Cano et al., (2012) showed that homotypic cannibalism by pancreatic adenocarcinoma (PDAC) cells was associated with upregulation of phagocytosis-related genes, such as TGF β . Furthermore, inactivation of ROCK1 did not prevent CIC formation in PDAC cells, but rather enhanced it, demonstrating that the molecular pathways driving cannibalism and entosis are not the same.

While RhoA-mediated contractility in invading inner cells drives entosis, increased tension within host cells could be implicated in cell cannibalism. Multiple mechanical forces are at play during phagocytic engulfment; notably an actin-mediated protrusive force to wrap around the particle, as well as plasma membrane and cortical tension which propel the particle inwards (Jaumouillé and Waterman, 2020). Given the similarity between the two processes, it is plausible that similar mechanics also drive cannibalism.

1.2.5. Implications of cell engulfment in cancer

The effects of CIC formation on cancer progression are complex and context dependent. While cannibalism and entosis can both result in division or escape of the internalised cell, most commonly this cell is degraded by host lysosomal enzymes (Fais and Overholtzer, 2018). The host cell can therefore benefit from additional nutrients to support its growth and contribute to tumour proliferation. For example, cannibalism has been shown to allow survival of metastatic melanoma cells following serum deprivation (Lugini et al., 2006). CIC formation has also been implicated in chemoresistance, potentially by shielding internalised cells from cytotoxic agents as well as environmental stressors. Supporting this, a recent study reported a negative correlation between CIC frequency and sensitivity to oxaliplatin and irinotecan across five colon cancer cell lines (Druzhkova et al., 2024). Furthermore, entotic engulfment can disrupt host cell division by interfering with

formation of the contractile ring, leading to cytokinesis failure and aneuploidy (Krajcovic et al., 2011). This promotes genomic instability, one of the key cancer hallmarks (Hanahan and Weinberg, 2011).

However, entosis has also been described as an anti-tumorigenic mechanism of clearing detached or misplaced cells before they acquire malignant potential (Guadamillas et al., 2011). Cannibalism can also have anti-tumorigenic effects; Cano et al., (2012) showed that PDAC patients with tumours exhibiting cannibalism develop fewer metastases than those without. Overall, it is clear that CIC formation has significant impacts on tumorigenesis, both positive and negative. However, ongoing research will be essential to gaining a comprehensive understanding of the implications of CIC in cancer.

1.3. Mutp53-dependent cell engulfment

Mackay et al., (2018) demonstrated that GOF mutp53 expression in cancer cells promotes the formation of CIC structures *in vitro*. CIC events are highest when mutp53 cells are co-cultured with either wtp53 or p53 KO cells, compared to single-cell cultures. Notably, mutp53 cells most often assume an engulfing cell fate, while p53 KO cells are internalised. This phenotype was observed across multiple mutp53-expressing cell lines, including A431 (epidermoid carcinoma), H1299 (non-small cell lung cancer), and HCT116 (colorectal carcinoma) cells. Furthermore, in lung adenocarcinoma patient samples, CIC frequency was highest in tumours with heterogeneous p53 expression, supporting the evidence *in vitro* that diversity in p53 expression may facilitate CIC formation. The same effect was observed in mouse xenograft models, with CIC-rich mutp53/KO co-cultures enhancing tumour growth.

1.3.1. Mechanisms of mutp53-dependent cell engulfment

While the presence of mutp53 in cancers is evidently linked with an increase in CIC formation, the exact mechanisms of mutp53-driven engulfment have not yet been elucidated. There is evidence for both cannibalism and entosis, but it is also possible that both processes are at play, or that a distinct, mutp53-specific mechanism may be responsible.

In support of entosis, Mackay et al. observed that engulfment of p53-null by mutp53 A431 cells was almost completely prevented when RhoA activity was impaired with a ROCK inhibitor. Furthermore, the authors detected increased β -catenin and E-cadherin (which mediate entotic cell-cell contacts) between host and internalised cells; this was not apparent in normal cell-cell junctions.

On the other hand, time-lapse imaging by Mackay et al. showed mutp53 A431 cells generating protrusions that extend around neighbouring cells, which were then engulfed. This would support cannibalism rather than entosis. Additionally, glucose starvation, which has previously been suggested to drive entosis (Hamann et al., 2017), did not promote CIC formation, but rather decreased it.

Further supporting cannibalism, mutp53 cells have been shown to engulf fixed, inactive cells, as well as large vesicles and beads (Dolma et al., 2025). Dolma et al. also examined the positioning of the Golgi body, which, in migrating cells, is usually orientated towards the leading edge (Millarte and Farhan, 2012). Within CIC structures, host cells orient their Golgi towards the cell that is being engulfed; however, internal cell Golgi are orientated in all directions, many away from the host. Collectively, these observations imply that mutp53 host cells drive CIC formation, pointing towards a cannibalistic rather than entotic mechanism.

1.3.2. Implications of mutp53-dependent cell engulfment

Mutp53-dependent cell engulfment has significant impacts on tumour progression. In p53-null hosts, cell engulfment tends to be anti-tumorigenic, as the presence of an internalised cell physically obstructs mitosis, resulting in host cell death. In contrast, mutp53 cells are frequently able to tolerate divisions despite having a cell internalised. However, this tolerance results in highly aberrant mitotic events, including tripolar divisions, cytokinesis failure, and multinucleation, which drive genomic instability and accumulation of oncogenic mutations. Evidencing this, Mackay et al. showed that in human lung adenocarcinomas, CIC frequency was positively correlated with mutp53 status and served as a predictor of poor patient outcomes. These findings highlight the importance of further investigating mutp53-dependent engulfment as a driver of tumour progression.

1.4. SH3BGRL protein

1.4.1. SH3BGRL structure and function

Src homology 3 domain binding glutamate rich protein like (SH3BGRL) is a 114-amino acid adaptor protein consisting of an SH3-binding domain and EVH1-binding domain (Egeo et al., 1998; Yin et al., 2005). SH3BGRL is expressed in lung, liver, placenta, heart, brain, pancreas, and skeletal muscle tissues, and is implicated in several key homeostatic processes, from signal trafficking to membrane transduction to cytoskeletal rearrangements (Li et al., 2020).

The roles of SH3BGRL in cancer are variable and context dependent. For instance, SH3BGRL can hyperactivate human epidermal growth factor receptor 2 (HER2) in breast cancers to induce therapeutic resistance (Li et al., 2020), whereas in lung cancer, SH3GRL has been shown to be important in tumour suppression (Liu et al., 2021). Furthermore, in acute myeloid leukaemia, SH3BGRL can exert both pro- and anti-tumorigenic effects (Xu et al., 2018; Yang et al., 2023), demonstrating that even within the same tumour type, the protein can behave differently. Overall, while the function of SH3BGRL in cancer remains contentious, it is clear that this is a key protein implicated in tumorigenesis.

1.4.2. SH3BGRL and mutp53

Dolma et al., (2025) identified SH3BGRL as a downstream target and binding partner of mutp53. In this context, SH3BGRL appears to be pro-tumorigenic. It is transcriptionally activated by mutp53 to promote CIC formation and also contributes to mutp53's GOF activity by enhancing etoposide resistance and anchorage-independent growth (independent of mutp53 expression). However, the extent to which these GOF effects are attributable to CIC formation remains unclear.

1.5. Cancer stemness

1.5.1. What are cancer stem cells?

Cancer stem cells (CSCs) are a small subpopulation of tumour cells characterised by their ability to self-renew and differentiate into multiple tumour cell types. As such, they play vital roles in driving tumour initiation and maintenance of heterogeneity (Zhao et al., 2017). CSCs can be identified based on the expression of specific cancer stemness markers, including CD133, CD44, SOX2, and ALDH1A1 (Zhao et al., 2017). They were first described in the 1990s in acute myeloid leukaemia (Bonnet and Dick, 1997), but have since been reported in a wide array of tumour types, including breast (Al-Hajj et al., 2003), colon (Ricci-Vitiani et al., 2007), lung, and bone cancers (Gibbs et al., 2005) to name a few.

The CSC model challenges traditional ideas of tumour heterogeneity, proposing a hierarchical organisation in which only this subset is able to regenerate the full diversity of tumour cell types (Rich, 2016). Beyond their role in tumour cell maintenance, CSCs have also been shown to drive several cancer hallmarks, including metastasis (Shiozawa et al., 2013), immune evasion (Lei and Lee, 2021), genomic instability (Liang et al., 2010), and chemoresistance (Abdullah and Chow, 2013). Furthermore, numerous studies have highlighted the plasticity of cancer stemness; for example, EMT can induce CSC phenotypes (Bocci et al., 2019), and non-CSC tumour cells can acquire stem-like properties following specific microenvironmental cues (Cabrera et al., 2015). Collectively, these findings highlight the importance of research into the biology of CSCs and the development of therapeutic strategies to effectively target this tumour population.

1.5.2. Mutant p53 and cancer stemness

Wtp53 typically inhibits the expression of CSC markers to prevent the acquisition of cancer stemness traits (Park et al., 2015). Conversely, one of the key GOF phenotypes of mutp53 is its ability to promote cancer stemness. This was first demonstrated by Sarig et al. (2010), who showed that mouse embryonic fibroblasts (MEFs) expressing mutp53 reprogrammed more efficiently than their p53 KO counterparts. *In vivo*, these mutp53-expressing cells gave rise to malignant tumours, while the p53 KO MEFs only formed teratomas, demonstrating that mutp53-induced stemness enhances oncogenic potential.

Mechanistically, mutp53 has been shown to transcriptionally activate cancer stemness markers to induce stem-like traits. For instance, in colorectal cancer, mutp53 binds to the promoter regions of ALDH1A1, Lgr5, and CD44 to expand CSC subpopulations (Solomon et al., 2018). As well as direct transcriptional regulation, mutp53 also promotes cancer stemness by inducing EMT, for example, via

regulation of miRNAs (Dong et al., 2013; Ghatak et al., 2021) or long non-coding RNAs (Zhao et al., 2019).

1.5.3. Cancer stemness and CIC formation

Although literature on cell engulfment and cancer stemness is limited, there is some evidence to suggest a direct association between the two processes. Notably, Chen et al. (2019) showed that aggressive breast cancer cells can engulf mesenchymal stem cells, leading to the transfer of stemness markers from internal to host cells. This suggests that CIC formation may be an active driver of stemlike traits in engulfing tumour cells. Moreover, given the similar abundance of engulfing cells and CSCs within tumours (both make up approximately 5%), it is plausible that CIC formation and cancer stemness are functionally linked.

1.6. Hypotheses and project aims

This thesis will investigate the mechanisms underlying mutp53-dependent CIC formation, based on three key hypotheses:

- 1. Firstly, our lab previously showed that mutp53 cells are prone to engulfing wtp53 or p53 KO cells (Mackay et al., 2018; Dolma et al., 2025). We hypothesise that this engulfment process is reminiscent of cannibalism rather than entosis. We also propose that CIC formation may depend on differences in plasma membrane tension between the host and internal cell.
- 2. Previous work in the lab identified SH3BGRL as a target gene of mutp53. It was hypothesised that SH3BGRL expression promotes cell engulfment, contributing to mutp53's GOF activity. A manuscript detailing these findings was under revision at the start of this MRes project and has since been published in *Cell Death Discovery* (Dolma et al., 2025).
- 3. Approximately 5% of cancer cells exhibit cell engulfment. A similar proportion of all cancer cells are CSCs. Engulfing cells and CSCs share similar traits, including enhanced chemoresistance and genomic instability; both are also associated with expression of mutp53. Collectively, these parallels led us to hypothesise that the engulfing cells represent the CSC population.

Based on these hypotheses, we established three aims, each addressed in separate chapters:

- 1. To characterise the mechanisms of mutp53-dependent cell engulfment, determining optimal methods for its detection (Chapter 3).
- 2. To further investigate the role of SH3BGRL in mutp53-dependent cell engulfment, and complete revision experiments for the manuscript submitted to *Cell Death Discovery* (*included as supplementary material to this thesis*) (Chapter 4).
- 3. To determine whether engulfing cells exhibit enhanced expression of cancer stemness markers (Chapter 5).

Chapter 2: Materials and Methods

2.1. Cell culture

2.1.1. Cell lines

A431 epidermoid carcinoma (CVCL_0037) cell lines were purchased from ATCC (LGC Standards). GFP-labelled telomerase-immortalised normal fibroblast cells (NFG) were gifted from the CRUK Scotland Institute, Glasgow.

Stable A431 p53 KO and mutp53 control cell lines were generated by Hannah Mackay, a previous student in the lab, using pre-made CRISPR constructs against p53 or an empty vector, plus lipofectamine 2000 reagent (Thermo Fisher Scientific). Fluorescent control and KO lines were established from these by transfecting with mCherry or GFP (2mg per well of a 6-well plate) (Addgene), then FACS-sorting for highly fluorescent cells (Mackay et al., 2018).

A431 mutp53 and p53 KO cell lines with stable SH3BGRL expression were generated by Lobsang Dolma in the lab (Dolma et al., 2025). This involved reverse transfection with human SH3BGRL gene (2μg per well of a 6-well plate) using lipofectamine 3000 (6 μl/well) and enhancer P3000 reagent (2μl/μg) (Thermo Fisher Scientific), followed by selection with hygromycin (Gibco, Thermo Fisher Scientific).

2.1.2. Routine cell culture

All cell lines were cultured in T75 flasks (Sarstedt) in Dulbecco's Modified Eagle Medium (DMEM), high glucose, pyruvate, and glutamine (Gibco, Thermo Fisher Scientific). Medium was supplemented with 10% foetal bovine serum (FBS) (Sigma-Aldrich). Cells were incubated at 37°C under 5% CO₂.

Cells were passaged twice weekly to maintain optimal growth conditions. Briefly, cells were washed with sterile phosphate-buffered saline (PBS) (Gibco, Thermo Fisher Scientific), then incubated at 37°C in 1.5ml trypsin for a few minutes until detached. Detached cells were resuspended in 8.5ml DMEM and seeded in a new T75 (typically at a dilution ratio of 1:20 to 1:30). Cells were regularly checked for contamination using an Evos XL Core microscope (Invitrogen) and confirmed to be mycoplasma-free.

2.1.3. Freezing and reviving cells

For cryopreservation, cells were washed, trypsinised, and resuspended as normal, then centrifuged at 1200rpm for 5 minutes. Cell pellets were resuspended in 1ml freezing medium (90% FBS, 10%

dimethyl sulfoxide (DMSO) (Tocris Bioscience)) per tube to be frozen, and transferred to cryogenic vials. Cryovials were initially stored at -80°C for a few days, then moved to -150°C for long-term storage.

To revive cells, cryovials were moved from -150°C to a 37°C water bath for 5 minutes. The thawed cell suspension was immediately transferred to a new T75 flask with 15ml DMEM plus 10% FBS and passaged the following day.

2.1.4. Co-culturing control and KO A431 cells for homotypic CIC formation

Cells were washed, trypsinised, and resuspended as normal, then transferred to 15ml Falcon tubes. $10\mu l$ of each cell suspension was added to a cell counting chamber slide and counted using the Counters 3 FL Automated Cell Counter (Invitrogen). Equal concentrations of control and KO cells $(1.2x10^5 \text{ of each per well of a 24-well plate})$ were seeded together and incubated at $37^{\circ}C$, 5% CO₂ for 24 hours to promote CIC formation.

2.2. Transient gene overexpression and knockdown

For transient overexpression, cells were reverse-transfected with 1µg plasmid DNA, 2µl P3000 enhancer reagent, and 3µl lipofectamine 3000 (Thermo Fisher Scientific) in 250µl serum-free medium per well of a 6-well plate.

For transient knockdown, cells were reverse-transfected with $1.5\mu l~20\mu M$ siRNA and $4.5\mu l$ Lipofectamine 3000 in 250 μl serum-free medium per well. SH3BGRL and non-targeting control siRNAs were purchased from Dharmacon.

For all reverse transfections, cells were seeded at a 1:4 ratio, and fresh medium added after 4 hours. To enhance knockdown or overexpression efficiency, an additional forward transfection (added dropwise) was performed the following day.

2.3. Confocal microscopy

2.3.1. Immunofluorescence staining for fixed confocal imaging

Cells were trypsinised and counted (see section 2.1.3), then seeded on coverslips in a 24-well plate at densities of 2.5×10^5 cells per well for single-cell cultures, or 1.25×10^5 of each cell line per well for CIC co-cultures.

After 24 hours, coverslips were washed twice in PBS, fixed in 4% paraformaldehyde (PFA) (Thermo Fisher Scientific) for 15 minutes at 4°C, then permeabilised in 0.1% Triton-X-100 (Sigma-Aldrich) (10 minutes, 4°C), and washed again in PBS.

Coverslips were blocked for one hour at room temperature in blocking buffer (2% bovine serum albumin (BSA), 1% donkey serum, 0.1% Tween-20, 22mg/ml glycine). Primary antibody incubation was performed in blocking buffer at the concentrations stated in Table 1, followed by secondary antibody at 1:250 (both incubations for one hour at room temperature).

For cytoskeletal staining, Phalloidin-647 (Abcam) was added to the secondary antibody mix (1:5000). Finally, coverslips were washed three times in PBS (5 minutes per wash), mounted in Vectashield Mounting Medium (+ DAPI) (Abcam), and sealed with nail varnish.

Table 1: Antibodies used for immunofluorescence staining.

Primary antibody	Species	Manufacturer	Concentration used
Anti-ALDH1A1	Rabbit	Cell Signalling Technology	1:100
Anti-DO-1	Mouse	Santa Cruz Biotechnology	1:150
Anti-RhoA	Rabbit	Abcam	1:100
Anti-SOX2	Rabbit	Abcam	1:100
Secondary antibody	Species	Manufacturer	Concentration used
Anti-mouse 488	Donkey	Abcam	1:250
Anti-rabbit 488	Donkey	Invitrogen	1:250
Anti-mouse 594	Donkey	Abcam	1:250
Anti-rabbit 594	Donkey	Invitrogen	1:250
Anti-mouse 633	Goat	Invitrogen	1:250
Anti-rabbit 647	Donkey	Abcam	1:250

2.3.2. Fixed confocal imaging to obtain CIC counts

Slides were imaged using the Zeiss 800 CLSM, and the Tile Scan function in Zen Blue was used to generate 25-36 images across each coverslip at 20x magnification.

CIC structures were identified and manually counted based on the following three criteria (Figure 2):

- 1. The host cell's nucleus is crescent shaped.
- 2. The internal cell is contained within a vacuole.
- 3. Both cells' nuclei are within the same focal plane.

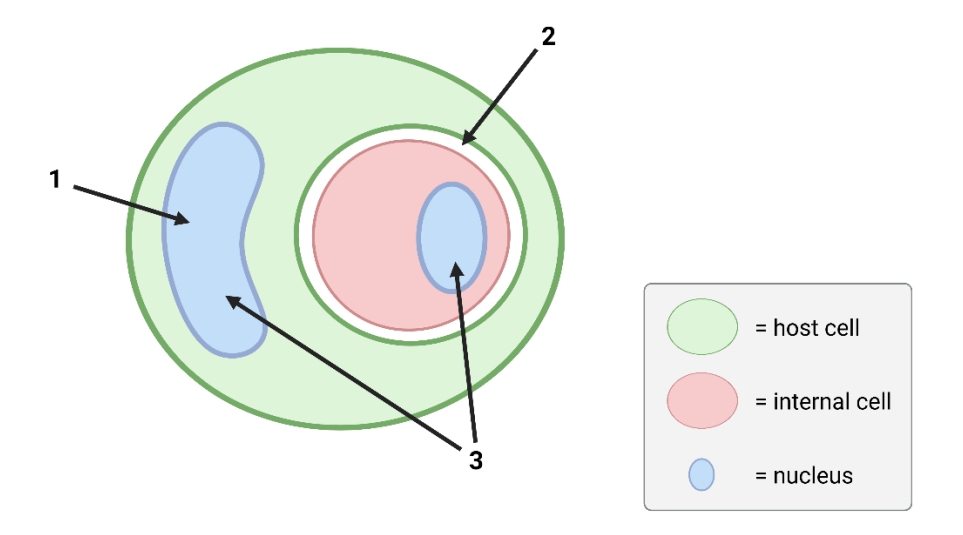


Figure 2: Three criteria for the identification of CIC structures in fixed confocal imaging.

1) The host cell (green) has a half-moon-shaped nucleus. 2) The internalised cell (red) is contained within a vacuole. 3) The nuclei (blue) of both cells are visible in the same focal plane. Made with BioRender.com.

CIC number was then normalised to the total number of cells, estimated by quantifying nuclei. Total nuclei counts were obtained using ImageJ. Firstly, auto-thresholding was applied to convert the DAPI channel images into binary format. The Binary Watershed function was then applied to resolve overlapping nuclei, delineating individual regions of interest (ROIs) (Figure 3). Finally, the Analyse Particles function was used to quantify total nuclear ROIs, with a minimum size threshold of 20 µm².

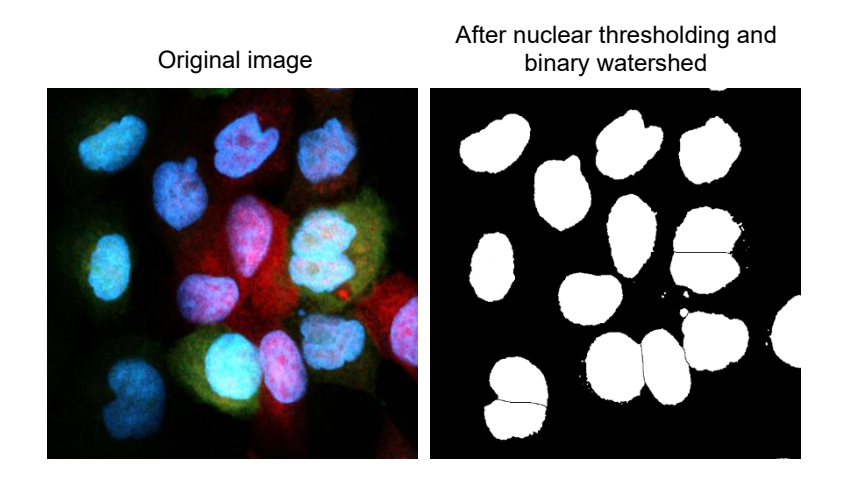


Figure 3: Thresholding nuclei for counting in Fiji (ImageJ).

DAPI channel images were first auto-thresholded to generate one-bit images. The Binary Watershed function was then used to separate overlapping nuclei into distinct regions of interest for quantification.

2.3.3. Fixed imaging of cells in suspension

Poly(2-hydroxyethyl methacrylate) (poly-HEMA) was used as a coating material for suspension cell culture. A 6 mg/mL solution of poly-HEMA (Sigma-Aldrich) was prepared in 95% ethanol and dissolved in a 65°C water bath. 500µl of the solution was then added to each well of a 24-well plate before incubating at 37°C to allow evaporation.

The following day, fluorescent cells were seeded onto the coated plates. Coverslips were added in after 5 hours of incubation, and cells gently pipetted on top. Coverslips were fixed in 4% PFA (10 minutes) and mounted in Vectashield for imaging on the Zeiss 800.

2.3.4. Incucyte live time-series imaging of CIC formation

The Incucyte® S3 Live-Cell Analysis System (Sartorius) was used for high-throughput live time-series imaging. Co-cultures of control and KO A431 cells stably expressing GFP or mCherry were seeded in a 96-well plate (1x10⁴ per well of each cell type). The cells were left to settle for 30 minutes before placing in the Incucyte incubator at 37°C and 5% CO₂. Images were taken at 20x magnification at 30-minute intervals over a period of 32 hours. Images were processed using the Incucyte Live Cell Analysis software.

2.3.5. Flipper-TR® fluorescence lifetime

Flipper-TR® (Spirochrome) is a fluorescent tension sensor that spontaneously integrates into plasma membranes. When the membrane is under tension, dithienothiophenes within the Flipper-TR probe align, resulting in a longer fluorescence lifetime. However, when the membrane is relaxed, these dithienothiophenes twist, shortening the fluorescence lifetime (Roffay et al., 2023). These variations can be detected with fluorescence lifetime imaging microscopy (FLIM).

To prepare for FLIM, cells were seeded in 35mm glass-bottom dishes at a density of 1.4x10⁵ cells per dish. After 48 hours, the cell medium was replaced with FluoroBrite™ DMEM (Gibco, Thermo Fisher Scientific) supplemented with FBS. Flipper-TR® (Spirochrome) was added at a concentration of 1mM, dissolved in DMSO. DMSO-only controls were also included to account for autofluorescence. Cells were incubated with the probe for 15 minutes at 37°C, 5% CO₂ before imaging.

Fluorescence lifetimes were measured using a Leica SP5 CLSM. Cells were maintained at 37°C, 5% CO₂ throughout imaging to ensure physiological conditions. A 488nm laser was used for excitation,

with emission detected between 575 and 800nm. FLIM tests were run until 1000 counts were reached, then fluorescence lifetimes (ns) recorded at 20 random positions along each cell membrane.

2.4. Western blot analysis

2.4.1. Cell lysis and protein extraction

Cells were washed twice in PBS then lysed on ice with NP40 lysis buffer (100mM NaCl, 100mM Tris pH-8, 1% NP-40) (75µl per well of a 6-well plate). Lysates were incubated on ice for 15 minutes then centrifuged at 14,000g for 15 minutes at 4°C. Supernatants were collected and combined with 4x sample buffer (1M Tris pH 6.8, 20% SDS, 20% glycerol, 10% beta-mercaptoethanol) then boiled for 5 minutes at 95°C. Lysates were used immediately for electrophoresis or stored at -20°C.

2.4.2. Sodium dodecyl-sulphate polyacrylamide gel electrophoresis (SDS-PAGE)

12% resolving gels (1.5M Tris pH 8.8, 40% Acrylamide/Bisphosphate, distilled H₂O, 10% SDS, 10% APS and TEMED) were casted using a hand cast system (Bio-Rad). A layer of butanol was added to create a level surface. After 30 minutes, the butanol was removed and the stacking gel (Tris-Cl pH 6.8, 40% Acrylamide/Bisphosphate, distilled H₂O, 20% SDS, 10% APS and TEMED) was poured with 1.5mm combs.

For a 10-well gel, 30µl lysate was loaded per well, and 5µl Precision Plus Protein[™] Dual Colour Standards used as a reference for protein size. Samples were run at 100V for one hour in SDS running buffer (5% MOPS (3-(N-morpholino)propanesulfonic acid) in distilled H₂O).

2.4.3. Protein transfer and immunoblotting

Proteins were transferred from the SDS gel onto a 0.5mm nitrocellulose membrane using a Wet electroblotting system (Bio-Rad). The system was run for 2 hours at 200mA in transfer buffer (10% Tris glycine, 20% methanol in distilled H₂O).

Membranes were then blocked in 5% skimmed milk in tris-buffered saline-tween 20 (TBST) for one hour at room temperature. Primary antibody incubation (*see Table 2 for concentrations*) was performed overnight at 4°C. Membranes were then washed three times in TBST and incubated in secondary antibody conjugated to a 680 or 800nm fluorophore (2 hours at room temperature, 1:20,000). Finally, membranes were washed a further three times and protein bands detected using the Odyssey Sa Infrared Imaging System (LI-COR).

Table 2: Antibodies used for immunoblotting.

Primary antibody	Species	Manufacturer	Concentration used
Anti-DO-1	Mouse	Santa Cruz Biotechnology	1:2000
Anti-GAPDH	Mouse	Proteintech	1:2000
Anti-RhoA	Rabbit	Abcam	1:500
Secondary antibody	Species	Manufacturer	Concentration used
Anti-mouse 680	Donkey	LI-COR IRDye®	1:20,000
Anti-rabbit 680	Donkey	LI-COR IRDye®	1:20,000
Anti-mouse 800	Donkey	LI-COR IRDye®	1:20,000
Anti-rabbit 800	Donkey	LI-COR IRDye®	1:20,000

2.5. Quantitative reverse transcription polymerase chain reaction (qRT-PCR)

2.5.1. RNA isolation

Cells were lysed and RNA extracted using the Total RNA Purification Kit (Norgen Biotek). Briefly, 350µl buffer RL was added to each well of a 6-well plate and incubated for 5 minutes. Lysates were collected in microcentrifuge tubes with 200µl 100% ethanol and vortexed before transferring to spin columns with collection tubes. Samples were centrifuged at 6000rpm for 1 minute and the flow-through discarded.

400μl wash solution A was then added and the samples spun for 1 minute at 14,000rpm, discarding flow-through. Samples were washed twice more in wash solution A, then the dry columns were spun for 2 minutes at 14,000rpm. Finally, 50μl elution solution A was added to the columns and the collection tubes replaced with fresh ones. To elute the RNAs, columns were spun for 2 minutes at 2000rpm, then 1 minute at 14,000rpm. RNA concentrations and purities were measured using a Nanodrop spectrophotometer, then stored at -20°C long-term.

2.5.2. cDNA synthesis

RNA samples were diluted to 500ng in 10µl nuclease-free water in PCR strip tubes. The Applied BiosystemsTM High-Capacity cDNA Reverse Transcription Kit (Thermo Fisher Scientific) was then used to prepare the RT master mix on ice (per sample: 2µl 10X RT Buffer, 0.8µl 25X dNTP Mix, 2µl 10X RT Random Primers, 1µl MultiScribe Reverse Transcriptase, and 4.2µl nuclease-free water). 10µl of master mix was added to each RNA sample, vortexing for 10 seconds. Controls of no RNA and no reverse transcriptase were also prepared.

The RNAs were reverse-transcribed into cDNA in a PTC-200 Peltier Thermal Cycler (10 minutes at 25°C, 2 hours at 37°C, 5 minutes at 85°C, and 4°C overnight). cDNA samples were diluted 1:20 in nuclease-free water for immediate use or long-term storage at -20°C.

2.5.3. qRT-PCR reaction

The Applied Biosystems PowerUpTM SYBRTM Green Master Mix (Thermo Fisher Scientific) was used for qRT-PCR. Enough master mix was prepared for 8µl per reaction plus one spare, and specific gene oligos (20µM) (Eurofins Genomics) (Table 3) were added at a concentration of 1/20th of the total master mix volume. 8µl of each cDNA sample was loaded into a 96-well PCR plate, with 8µl master mix pipetted on the other side of the well. For each sample, GAPDH was used as a reference gene.

Table 3: Primers used for qRT-PCR. Reverse

Forward GAGGTTGGCTCTGACTGTAC CCGTCCCAGTAGATTACCAC p53 SH3BGRL CTGGCTCTACAGCGATTAAGAA TGGCTGGTCGACTATTTTCAGL GAPDH GCAGAGATGATGACCCTTTTGGCT TGAAGCTCGGAGTCAACGGATTGGT

The plate was sealed with adhesive film and spun down at 200g for 1 minute. The CFX Duet Real-Time PCR System (Bio-Rad) was then used for detection. From raw CT values, fold changes in RNA expression were calculated using the following equations:

$$\Delta CT = CT \text{ (target gene)} - CT \text{ (reference gene (GAPDH))}$$

 $\Delta \Delta CT = \Delta CT \text{ (target sample)} - \Delta CT \text{ (reference sample)}$

2.6. Soft agar colony formation assay

Control and KO A431 cells were co-cultured for 24 hours to allow for CIC formation. 2ml of autoclaved 0.5% agar (low gelling temperature agarose (Sigma-Aldrich) in PBS) was then added to each well of a 6-well plate and allowed to set for 30 minutes at room temperature. 2x10⁴ cells from each co-culture in 750µl media were combined with 750µl 0.8% agar (kept in a water bath at 42°C) and added dropwise to the plate.

Cells were then incubated for 14 days to allow single colonies to grow and refreshed with 750µl medium on day 5. On day 19, plates were incubated in 60µl crystal violet (0.025% in 20% methanol) on a shaker for 1 hour at room temperature. Plates were imaged using the Odyssey Sa Infrared Imaging System (LI-COR) and colonies counted using the Analyse Particles function in ImageJ.

2.7. Statistical analysis

Statistical analysis and graphing was performed in RStudio or GraphPad Prism. Data were expressed as means plus or minus standard deviation or standard error of the mean. For data sets with small sample sizes (e.g. n = 3), normal distribution was assumed. Unpaired and paired student's t-tests were applied where appropriate; notably, a paired t-test was used to compare FLIM measurements between engulfing and internal cells within CIC structures. Finally, for the colony formation assay, a two-way ANOVA was used to assess the effects of two independent variables across multiple groups.

Chapter 3: Characterisation of mutant-p53-dependent cell engulfment

3.1. Introduction and aims

The initial aim for this MRes project was to characterise the mechanisms underlying cell engulfment in mutp53 cancer cells. Prior work in our lab (Mackay and Muller, 2019; Dolma et al., 2025) has provided evidence for both cannibalism and entosis. We hypothesised that mutp53-driven engulfment, while potentially its own distinct mechanism, is most closely aligned with cannibalism.

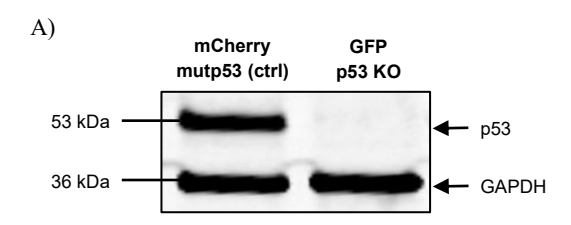
Given the limited understanding of the molecular mechanisms underlying cannibalism, we instead aimed to eliminate entosis by investigating two implicated factors: RhoA expression and differential plasma membrane tension. Before investigating mechanistic details, we first established optimal conditions for observing engulfment in A431 (epidermoid carcinoma) cells, including time points, seeding density, and adherent versus suspension cultures.

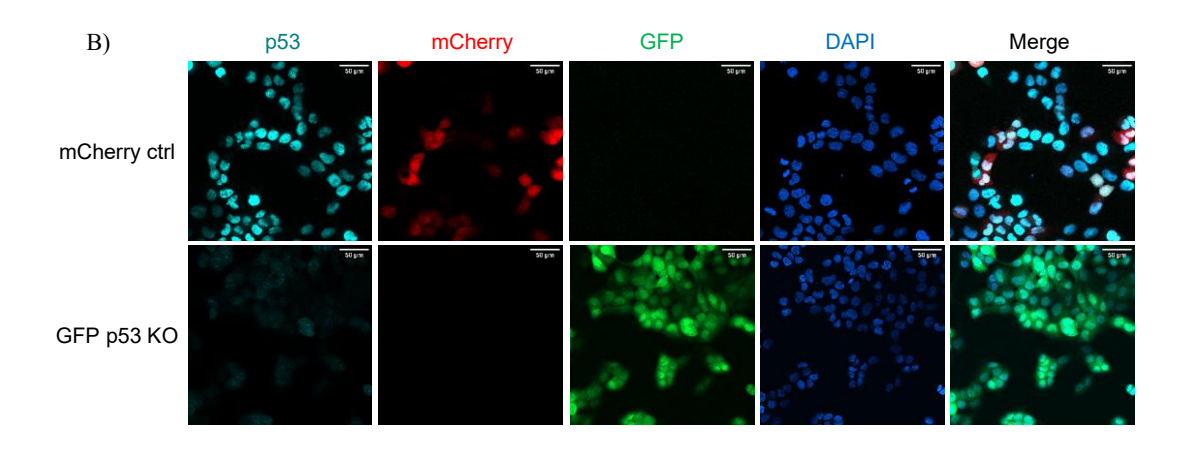
3.2. Results

3.2.1. Validation of A431s as a model system for studying CIC formation

Our lab previously demonstrated that cell engulfment by mutp53 (control) cells is most frequent when co-cultured with p53 KO cells. Stable A431 control and KO lines were established by Hannah Mackay, a former student in the lab (Mackay et al., 2018). GFP or mCherry were also stably transfected in so that the two cell types could be easily distinguished in immunofluorescence experiments.

At the start of this project, p53 expression in these cell lines was assessed via western blotting, and confocal microscopy used to verify mCherry/GFP expression (Figures 4A and 4B). Co-culturing the two cell types in equal concentrations for 24 hours led to frequent CIC formation, as observed via immunofluorescence (Figures 4C and 4D). Moreover, mCherry control cells more often engulfed p53 KO cells than the reverse, solidifying the role of mutp53 in driving cell engulfment.





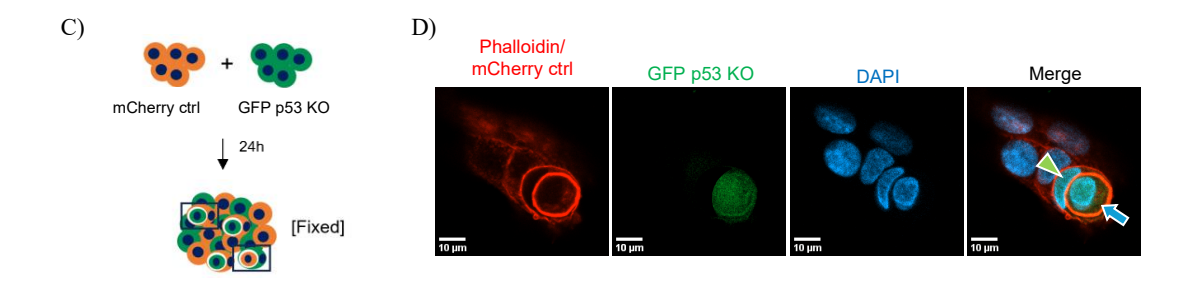


Figure 4: Validation of A431s as a model system for studying CIC formation.

A) Western blot for p53 expression in mCherry control cells (mutp53 R273H) versus CRISPR p53 GFP KO cells. GAPDH was used as a loading control. B) Representative confocal images showing distinct expression of mCherry in control cells and GFP in p53 KO cells. Immunofluorescence staining for p53 (cyan) shows strong nuclear expression in control cells and minimal expression in KO cells, consistent with successful knockout. Scale bar = 50μm. C) Schematic of CIC co-culture setup: equal concentrations of mCherry and GFP KO cells were seeded, then incubated for 24 hours and fixed for confocal imaging. Adapted from Dolma et al., (2025). D) Representative confocal image of a CIC structure, showing a p53 KO cell (blue arrow) internalised within a control cell (green arrow). Scale bar = 10μm.

3.2.2. Optimising conditions for observing mutp53-dependent CIC formation in vitro

CIC events can be transient and rely on cell-cell proximity, so careful timing is essential to optimising their observation *in vitro*. To determine the best time points for observing CIC formation, we used the Incucyte system for high-throughput live cell imaging. Three concentrations of GFP control/mCherry p53 KO co-cultures were seeded in a 96-well plate and imaged over a period of 32 hours. CIC structures were quantified in each field of view at 4-hour intervals.

Our previous immunofluorescence protocol for CIC formation involved harvesting and fixing cells 24 hours after seeding. The Incucyte data showed that CIC number increases steadily until around 16 hours post-seeding, but begins to decrease at around 24 hours (Figure 5). Co-cultures should therefore be harvested within the 16- to 24-hour window to maximise CIC counts.

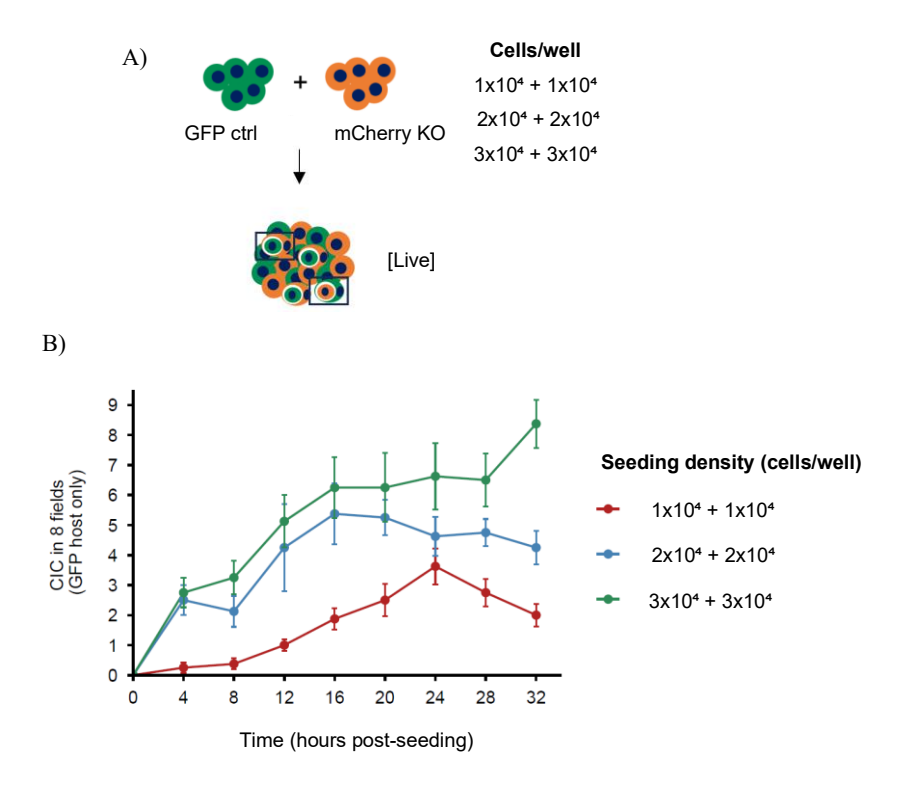


Figure 5: Determining the optimum time frame for observing cell engulfment.

A) Schematic of CIC co-culture setup: three concentrations of GFP control and mCherry KO A431 cells were seeded in a 96-well plate and placed in the Incucyte system for live cell imaging. B) For each seeding density, the number of CIC structures is greatest between approximately 16 and 24 hours post-seeding (n = 8, error bars = SEM).

We next tested out a cell suspension protocol in which plates were coated with poly(2-hydroxyethyl methacrylate) (poly(HEMA)) prior to cell seeding. This approach has been shown to facilitate entosis by mimicking loss of ECM attachment (Sun and Overholtzer, 2013).

Co-culturing mCherry control and GFP KO cells on poly(HEMA) plates did yield clearly defined, rounded CIC structures in fixed confocal imaging (Figure 6). However, it is unclear whether poly(HEMA) promotes mutp53-driven engulfment, or instead enhances a distinct, entosis-like mechanism. Furthermore, the protocol raised technical difficulties during fixation, as cells tended to aggregate tightly and were difficult to aspirate. These clumps also impeded live-cell imaging, with the DNA stain Hoechst failing to integrate effectively into densely packed cells. For these reasons, it was decided not to continue with poly(HEMA) coating beyond this experiment.

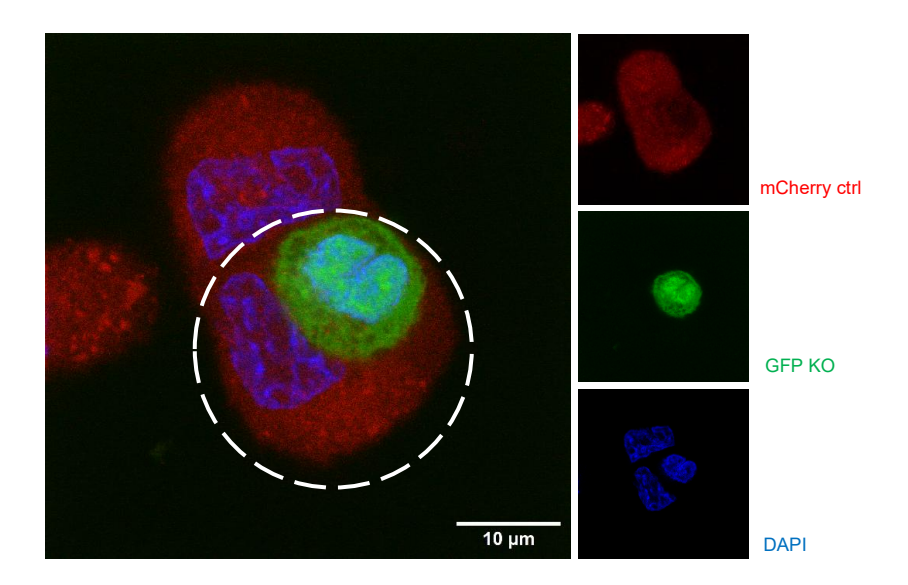


Figure 6: CIC formation can be observed in fixed suspension cultures.

Representative confocal image of a GFP KO cell internalised within an mCherry control cell (white circle annotation). Fluorescent cells were seeded in poly(HEMA)-coated suspension plates then fixed and mounted for imaging. Scale bar = $10\mu m$.

3.2.3. Mutp53-driven engulfment is reminiscent of cannibalism rather than entosis
In order to observe the engulfment process, we used the Incucyte system for high-throughput live time-series imaging. GFP control and mCherry KO cells were co-seeded in a 96-well plate and immediately placed in the Incucyte, with images taken every 30 minutes over a 32-hour period.

Consistent with our previous findings (Figure 5), most CIC events were observed within the 16- to 24-hour window. Notably, GFP control host cells were most often driving the process, extending phagocytic-like protrusions to wrap around and internalise KO cells (Figure 7). This reinforces our hypothesis that mutp53-dependent engulfment more closely resembles cannibalism than entosis.

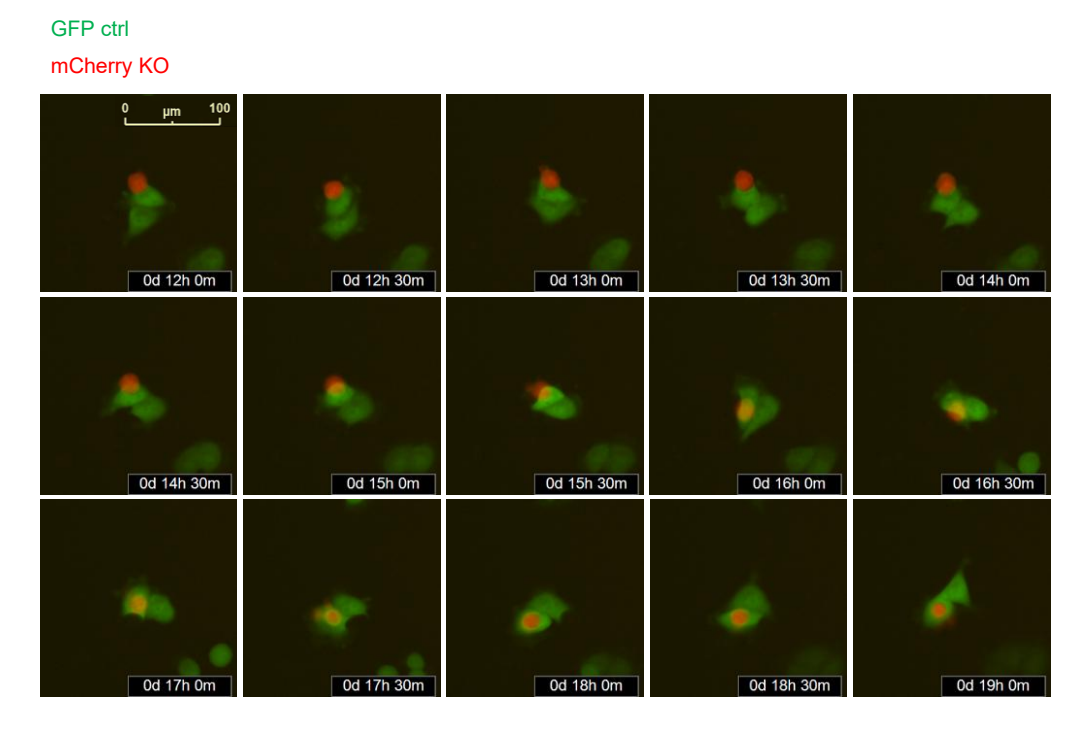


Figure 7: Live time-series imaging of mutant-p53-driven cell engulfment.

Incucyte time-series imaging of CIC formation in GFP control and mCherry KO A431 co-cultures. Time points represent hours post-seeding, with images taken at 30-minute intervals. A GFP cell can be seen wrapping around the mCherry cell, which is fully internalised by around 18 hours after establishing the co-culture.

To further rule out entosis as the mechanism of mutp53-dependent CIC formation, we examined RhoA expression in mutp53 versus KO cells. Previous studies have reported elevated RhoA in invading entotic cells (Sun et al., 2014; Durgan et al., 2017). If entosis underlies mutp53-dependent CIC formation, higher RhoA levels should therefore be expected in p53 KO cells, as these predominantly adopt an internal cell fate.

RhoA expression was assessed by confocal microscopy and western blotting (Figure 8). RhoA-GFP was also overexpressed in control cells to confirm the antibody was working, and a secondary antibody-only negative control was included to establish baseline fluorescence levels for confocal imaging. Overall, no clear differences in RhoA levels were observed; this points towards cannibalism rather than entosis as we hypothesised. However, further experiments will be needed to investigate whether CIC formation may induce changes in RhoA expression, rather than mutp53 and KO cells having inherently different RhoA levels.

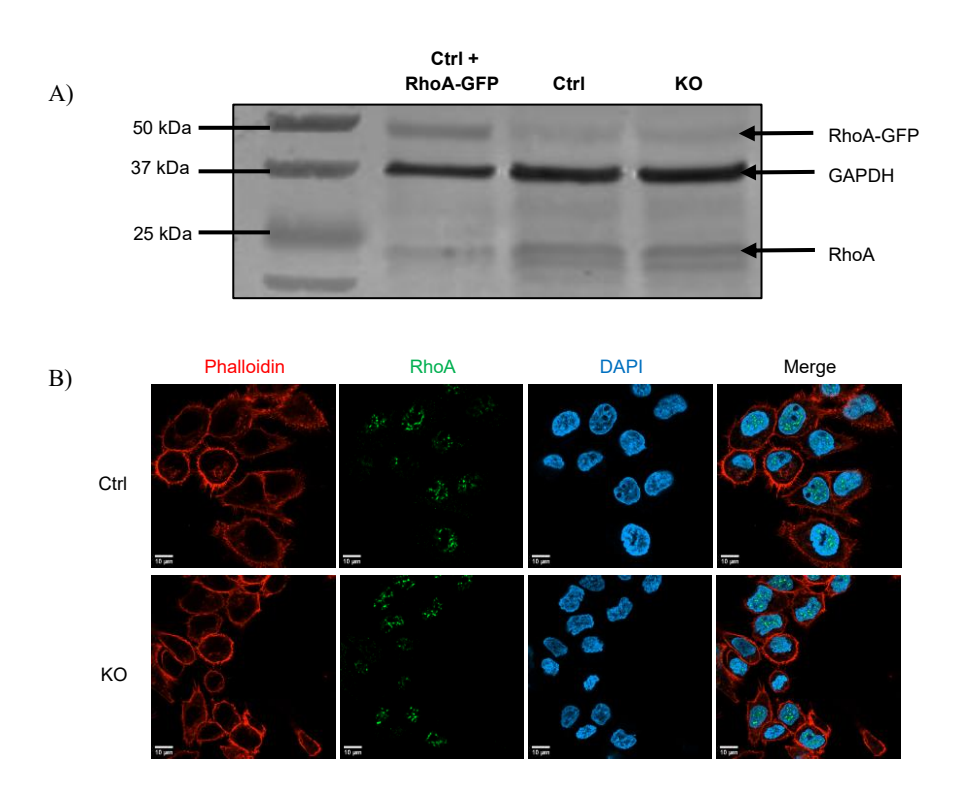


Figure 8: RhoA expression in mutp53 versus p53 KO cells.

A) Western blot for RhoA in control and p53 KO A431 cells, with GAPDH as a loading control. RhoA-GFP was additionally expressed in control cells to validate antibody specificity. B) Representative confocal images of RhoA staining in control and KO cells using rabbit anti-RhoA (1:100) and Alexa Fluor 488-conjugated donkey anti-rabbit (1:250) antibodies. Scale bar = $10\mu m$.

3.2.4. Differences in plasma membrane tension are apparent within CIC structures

Mechanistically, both entosis and cannibalism are thought to rely on differences in tension between host and internal cells. We were therefore interested in investigating whether mutp53 and KO cells exhibit intrinsic differences in membrane tension, and whether this is important in determining host versus internal cell fate in CIC structures.

To quantitatively assess membrane tension, we performed fluorescence lifetime imaging microscopy (FLIM) using Flipper-TR®. Flipper-TR is a mechanosensitive probe that spontaneously integrates into plasma membranes. Under increased tension, dithienothiophenes within the probe align, prolonging fluorescence lifetime. Conversely, relaxed membranes induce twisting of these moieties, shortening the lifetime of the probe (Roffay et al., 2023).

Before establishing co-cultures for CIC formation, we first analysed individual cultures of mutp53 and p53 KO A431s and saw no differences in fluorescence lifetime between the two cell types (Figure 9.1). On the other hand, fluorescence lifetime was significantly longer in engulfing versus internalised cells within CIC structures (Figure 9.2). Collectively, these observations imply that membrane tension differences are not inherent to mutp53 versus KO cells, but rather CIC formation induces these changes.

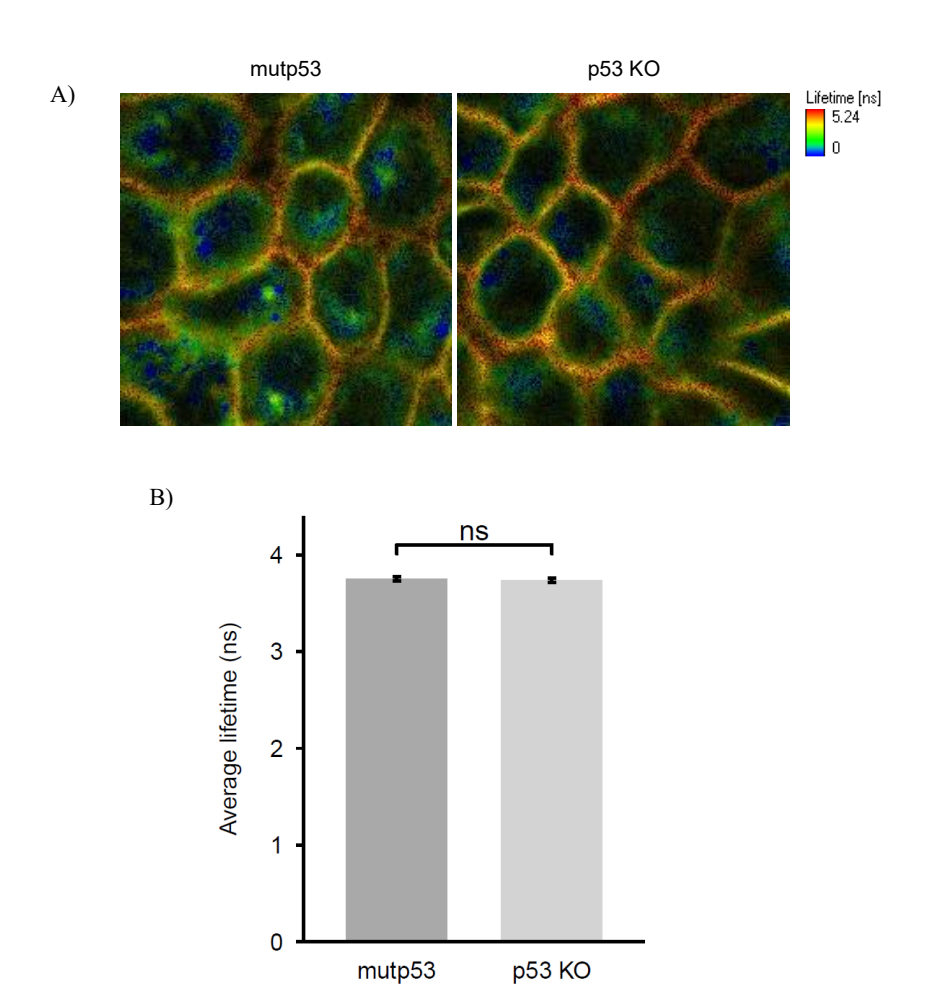
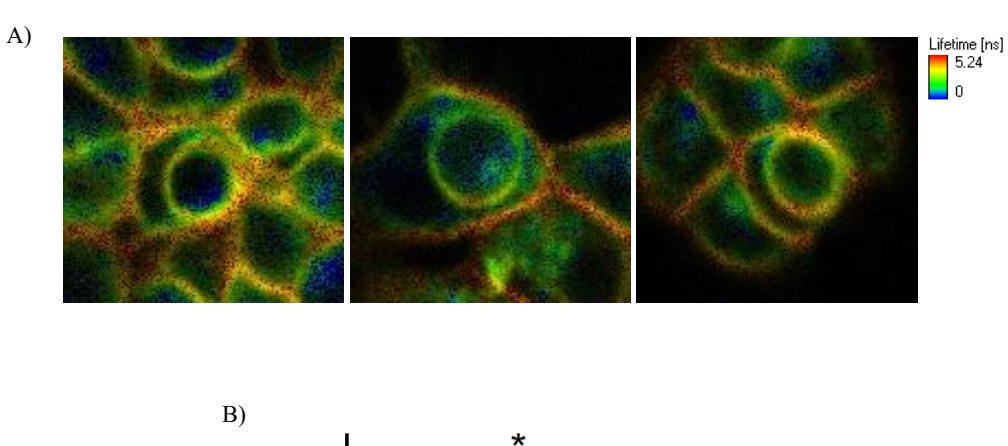


Figure 9.1: Membrane tension in mutp53 versus p53 KO A431 cells.

A) FLIM images using the Flipper-TR probe showing membrane tension within A431 mutp53 versus p53 KO cultures. Longer fluorescence lifetimes indicate greater membrane tension. B) No significant differences in membrane tension were detected between mutp53 and p53 KO cells. For each cell, 20 lifetime measurements were taken at random positions along the membrane (n = 5, unpaired t-test, $*p \le 0.05$, error bars = SEM).



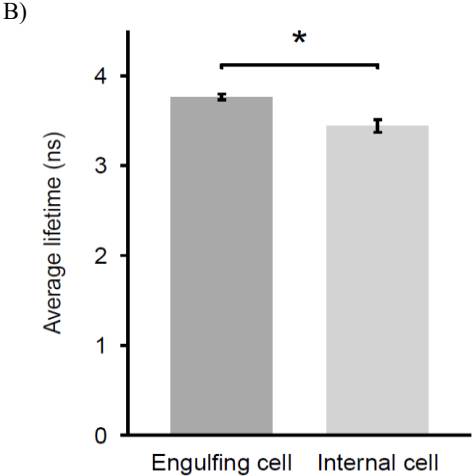


Figure 9.2: Differences in membrane tension between engulfing and internal cells.

A) FLIM images using the Flipper-TR probe showing differences in membrane tension within A431 mutp53 CIC structures. Longer fluorescence lifetimes indicate greater membrane tension. B) Engulfing cell membranes showed significantly higher average fluorescence lifetimes than the membranes of internalised cells. For each cell, 20 lifetime measurements were taken at random positions along each membrane (n = 3, paired t-test, $*p \le 0.05$, error bars = SEM).

3.3. Discussion

After optimising conditions for observing CIC structures *in vitro*, this chapter focused on exploring the mechanisms of mutp53-dependent engulfment, based on the two existing models of entosis and cannibalism. Live imaging from the Incucyte showed that engulfing cells were consistently more active than internal cells during CIC formation, extending phagocytic-like protrusions (Figure 7). These behaviours reinforce our hypothesis that mutp53-driven engulfment resembles a cannibalistic process. Supporting this interpretation, we found no inherent differences in RhoA expression between mutp53 and KO cells (Figure 8). Given RhoA's central role in driving inner cell invasion during entosis (Sun et al., 2014), this suggests that mutp53-driven CIC formation may occur via a non-entotic route.

Upregulation of RhoA is important in invading entotic cells as it generates the contractile force and increased cortical tension needed to push the cell into its neighbour (Overholtzer et al., 2007). However, even if mutp53-driven engulfment is cannibalistic, differences in tension may still be at play. Several studies have implicated increased plasma membrane tension in phagocytic cells as a driver of engulfment (Masters et al., 2013; Jaumouillé and Waterman, 2020). Given the mechanistic parallels between cannibalism and phagocytosis, it is therefore plausible that membrane tension would be increased in engulfing mutp53 cells.

While our FLIM data showed no differences in membrane tension between individual cultures of mutp53 and KO cells, we did see significantly higher tension in engulfing cell membranes (Figure 9.2). In other words, CIC formation seems to be inducing changes in membrane tension, with the increase in engulfing cells suggesting a cannibalistic or phagocytic-like mechanism. Perhaps RhoA expression is therefore also context-dependent, becoming upregulated in engulfing cells to increase membrane tension. Further immunofluorescence experiments, or live imaging with a fluorescent RhoA reporter, could help to determine whether RhoA is enriched during CIC formation.

Ideally, FLIM data should be captured during the earlier stages of CIC formation. This could reveal whether differences in membrane tension play a role in initiating engulfment, and whether tensions vary throughout the engulfment process. However, early CIC structures can be easily mistaken for neighbouring or overlapping cells. To address this, Hoechst live DNA stain could be used to visualise the crescent-shaped nuclei that are characteristic of engulfing cells.

Another important consideration is whether the Flipper probe is binding specifically to the inner cell membrane or to the vesicle that encloses it. To clarify this, p53 KO cells could be incubated with the

probe prior to co-culture with mutp53 cells, so only the KO cell membranes are labelled. Transmitted light could then be used to identify CIC structures, and FLIM lifetimes of internalised versus non-CIC KO cells compared.

Chapter 4: The role of SH3BGRL in mutant p53-dependent cell engulfment

4.1. Introduction and aims

One of the aims for this MRes project was to help complete revisions for a manuscript (Dolma et al., 2025 – *included as supplementary material to this thesis*) detailing the role of SH3BGRL, a target gene of mutp53, in driving CIC formation. The reviewers requested experiments investigating the effect of SH3BGRL silencing on CIC formation, and the contribution of SH3BGRL to mutp53 GOF phenotypes such as anchorage-independent growth.

4.2. Results

4.2.1. Loss or overexpression of SH3BGRL affects the frequency of CIC formation

The original manuscript showed SH3BGRL to be enriched in host versus internal cells within CIC structures, indicating a role in promoting cell engulfment. To more directly address this, the reviewers were interested in whether the ability of mutp53 cells to engulf is compromised following SH3BGRL silencing.

We therefore assessed the impact of transient SH3BGRL knockdown on CIC formation using fixed confocal imaging. GFP mutp53 cells were reverse transfected with SH3BGRL siRNA or a non-targeting control, and co-cultured with mCherry KO cells the following day to promote CIC formation. After a further 24 hours, co-cultures were fixed and mounted for confocal imaging. Quantitation in ImageJ showed that loss of SH3BGRL in control cells significantly reduced CIC formation (Figure 10.1).

Additionally, KO cells were co-cultured with control cells stably over-expressing SH3BGRL. This resulted in a marked increase in CIC frequency versus normal control/KO co-cultures (Figure 10.2). Together, these findings support a functional role for SH3BGRL in driving mutp53-dependent engulfment.

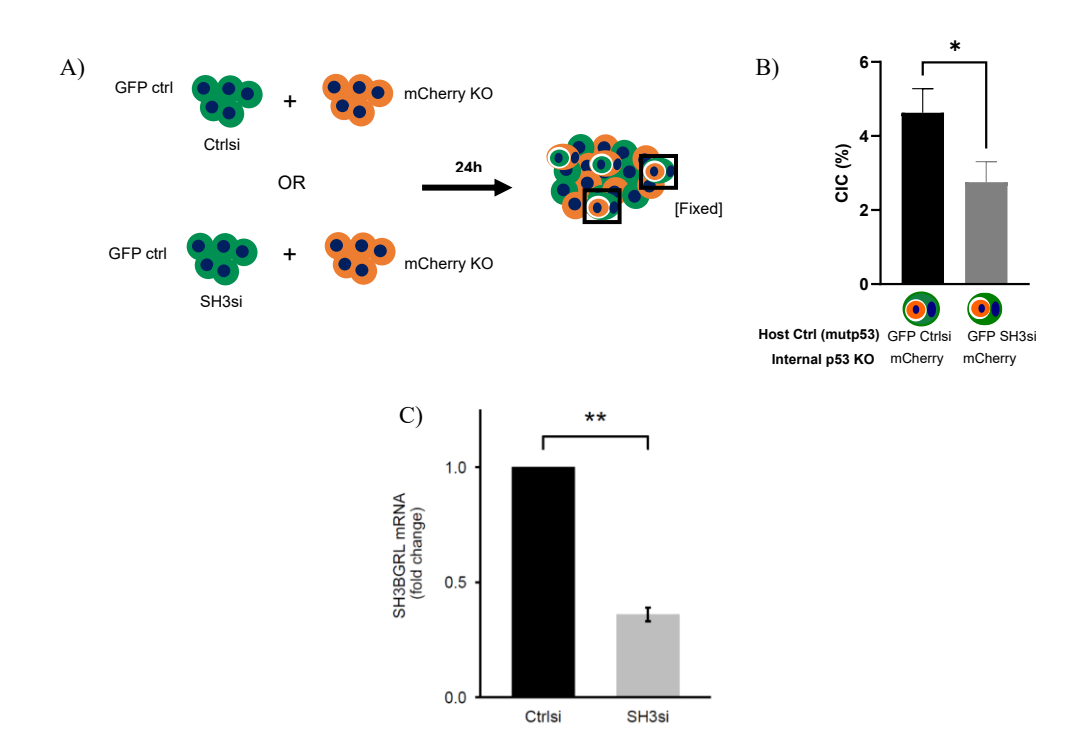


Figure 10.1: Transient SH3BGRL knockdown in control cells reduces mutp53-driven CIC formation.

A) Schematic of CIC co-culture setup: GFP control A431 cells were transfected with SH3BGRL siRNA or a non-targeting control siRNA, then combined with mCherry KO cells. Co-cultures were incubated for 24 hours and fixed for confocal imaging. B) Loss of SH3BGRL in control cells significantly reduces the percentage of cells forming CIC structures (n = 36, student's t-test, *p ≤ 0.05, error bars = SEM). Adapted from Dolma et al., 2025. C) qPCR analysis of SH3BGRL mRNA expression in GFP control cells transfected with either control or SH3BGRL siRNA. Transfection efficiency was confirmed (n = 3, student's t-test, **p ≤ 0.01, error bars = SEM).

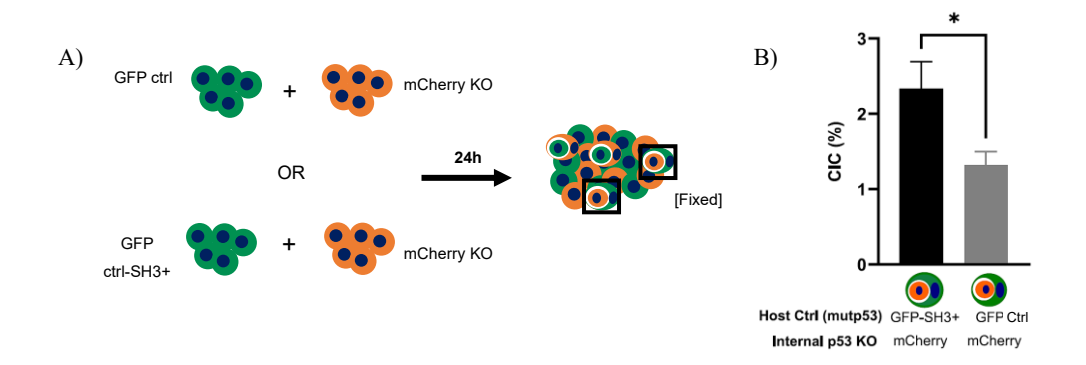


Figure 10.2: Stable SH3BGRL overexpression in control cells promotes mutp53-driven CIC formation.

A) Schematic of CIC co-culture setup: mCherry KO A431 cells were combined with either GFP control cells or GFP control cells stably overexpressing SH3BGRL. Co-cultures were incubated for 24 hours and fixed for confocal imaging. B) Overexpression of SH3BGRL in control cells significantly increases the percentage of all cells forming CIC structures (n = 36, student's t-test, $*p \le 0.05$, error bars = SEM). Adapted from Dolma et al., 2025.

4.2.2. SH3BGRL expression promotes anchorage-independent growth

Anchorage-independent growth refers to the ability of cells to proliferate without adhesion to the ECM. This is vital in facilitating metastasis, as it enables cells to disseminate throughout the body and colonise distant sites. It also confers resistance to anoikis, a form of apoptosis that eliminates displaced cells, allowing these metastatic cells to continue to survive despite the absence of ECM attachment (Guadamillas et al., 2011).

Anchorage-independent growth can be assessed *in vitro* using a soft agar colony formation assay (Du et al., 2017). A layer of agar is first poured into the plate and allowed to solidify, before adding a second layer of agar with a specific number of cells. The plate is incubated for two weeks, after which the number of colonies can be counted to give an estimation of cell malignancy.

The paper had already shown that mutp53 A431 cells exhibit greater agar colony formation than p53 KO cells (Dolma et al., 2025). Stable SH3BGRL overexpression further enhanced colony formation in both mutp53 and KO cells. Overall, this implies that both mutp53 and SH3BGRL are drivers of anchorage-independent growth.

To address whether mutp53 regulates anchorage independent growth via SH3BGRL regulation, we performed transient siRNA knockdown of SH3BGRL in mutp53 cells prior to seeding in agar. Colony formation was significantly reduced with SH3BGRL knockdown, solidifying the role of SH3BGRL in promoting anchorage-independent growth, and suggesting that mutp53 regulates SH3BGRL expression to drive this phenotype (Figure 11).

We also set up co-cultures incorporating p53 KO cells to assess whether CIC formation promotes anchorage-independent growth. As with the single-cell cultures, colony formation was significantly reduced when SH3BGRL was knocked down in mutp53 cells. However, colony numbers were not significantly different in the CIC co-cultures relative to single-cell cultures. This may be explained by the low seeding density required for this assay, reducing the likelihood of CIC events. Moreover, the presence of KO cells in the co-culture, which themselves are less prone to anchorage-independent growth, may have reduced the number of colonies formed.

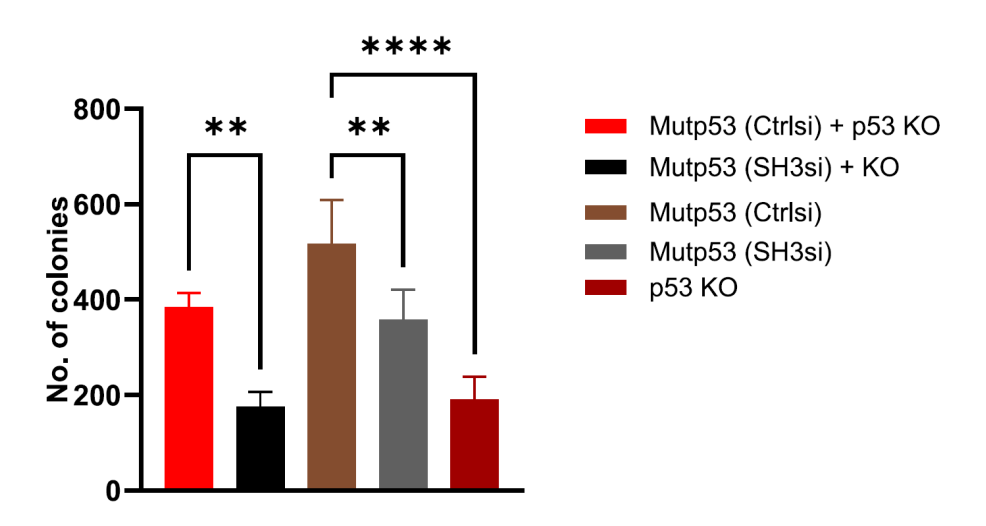


Figure 11: Transient knockdown of SH3BGRL in mutp53 cells significantly reduces soft agar colony formation.

Number of colonies formed in soft agar assay (n = 3, two-way ANOVA, $*p \le 0.05$, $**p \le 0.01$, $***p \le 0.001$, error bars = SD). A431 control cells were treated with SH3BGRL siRNA or a non-targeting control siRNA. After 24 hours, the treated control cells were seeded in agar, either alone, or in co-culture with p53 KO cells to promote engulfment. The agar plates were then incubated for two weeks before counting colonies. Adapted from Dolma et al., 2025.

4.3. Discussion

The original Dolma et al. manuscript described CIC formation as a process driven by host mutp53 cells, which transcriptionally induce SH3BGRL expression to facilitate engulfment. Supporting this, we showed through confocal imaging and CIC quantification that overexpression or silencing of SH3BGRL significantly impacts the ability of mutp53 cells to engulf (Figure 10.1, Figure 10.2).

We also demonstrated that transient SH3BGRL silencing in mutp53 cells reduces their capacity to form colonies in soft agar (Figure 11). This supported existing evidence from the paper that mutp53 may regulate SH3BGRL to promote anchorage-independent growth, offering a distinct advantage to tumour cells in terms of survival and dissemination.

A key unresolved question was whether CIC formation itself promotes anchorage-independent growth, or if this is simply a GOF effect of mutp53 driven by SH3BGRL. It has been hypothesised that CIC formation, particularly entosis, may offer a mechanism for tumour cells to escape anoikis and grow anchorage-independently (Guadamillas et al., 2011). However, the colony formation assay was deemed insufficient to address this, as the seeding density required was too low to support robust CIC formation. Furthermore, CIC events are inherently transient, making it difficult to capture their effects in long-term assays. If this experiment were to be repeated, it may therefore be worthwhile to used FACS-sorted CIC populations to enrich for cells actively undergoing, or having undergone engulfment.

It is also important to note that SH3BGRL expression and function can vary markedly across tumour types. For instance, it is upregulated in breast and oral cancers, yet downregulated in liver cancer (H. Wang et al., 2016; Saleh et al., 2023). Moreover, even within a single cancer type, SH3BGRL can have both tumour-suppressing and tumour-promoting functions, as demonstrated in acute myeloid leukaemia (Xu et al., 2018; Yang et al., 2023). Further work in a variety of cell lines will therefore be important in gaining a comprehensive understanding of the role of SH3BGRL in mutp53-dependent engulfment.

Chapter 5: CIC formation is associated with expression of cancer stemness markers

5.1. Introduction and aims

Cancer stemness confers a significant advantage to tumour cells, enabling self-renewal and multilineage differentiation. These properties underpin tumour initiation, drive proliferation, and contribute to resistance against conventional therapies. As with normal stem cells, CSCs can be identified based on expression of specific stemness markers. Examples of these include SOX2, a transcription factor and master regulator of pluripotency, and ALDH1A1, which regulates cell self-protection and differentiation (Zhao et al., 2017).

Despite their significant impacts on tumorigenesis, CSCs only make up around 5% of all cancer cells (Li et al., 2007). Intriguingly, approximately 5% of cancer cells also undergo CIC formation. This raises the question as to whether the CIC-forming cells represent the CSC population. We therefore set out to assess for cancer stemness, via immunofluorescence staining for SOX2 and ALDH1A1, in mutp53 cells and subsequently CIC structures.

5.2. Results

5.2.1. Mutp53 cells express cancer stemness markers

Before looking at CIC structures, we firstly examined CSC marker expression in our A431 mutp53 versus p53 KO cells. Cells were fixed and stained via immunofluorescence for SOX2 or ALDH1A1. A secondary antibody-only negative control was used to define baseline fluorescence, and the same laser settings were applied across all images to ensure consistency.

Expression of SOX2 was appeared higher in the mutp53 cell cultures, whereas ALDH1A1 was more similarly expressed in control and KO cells (Figure 12).

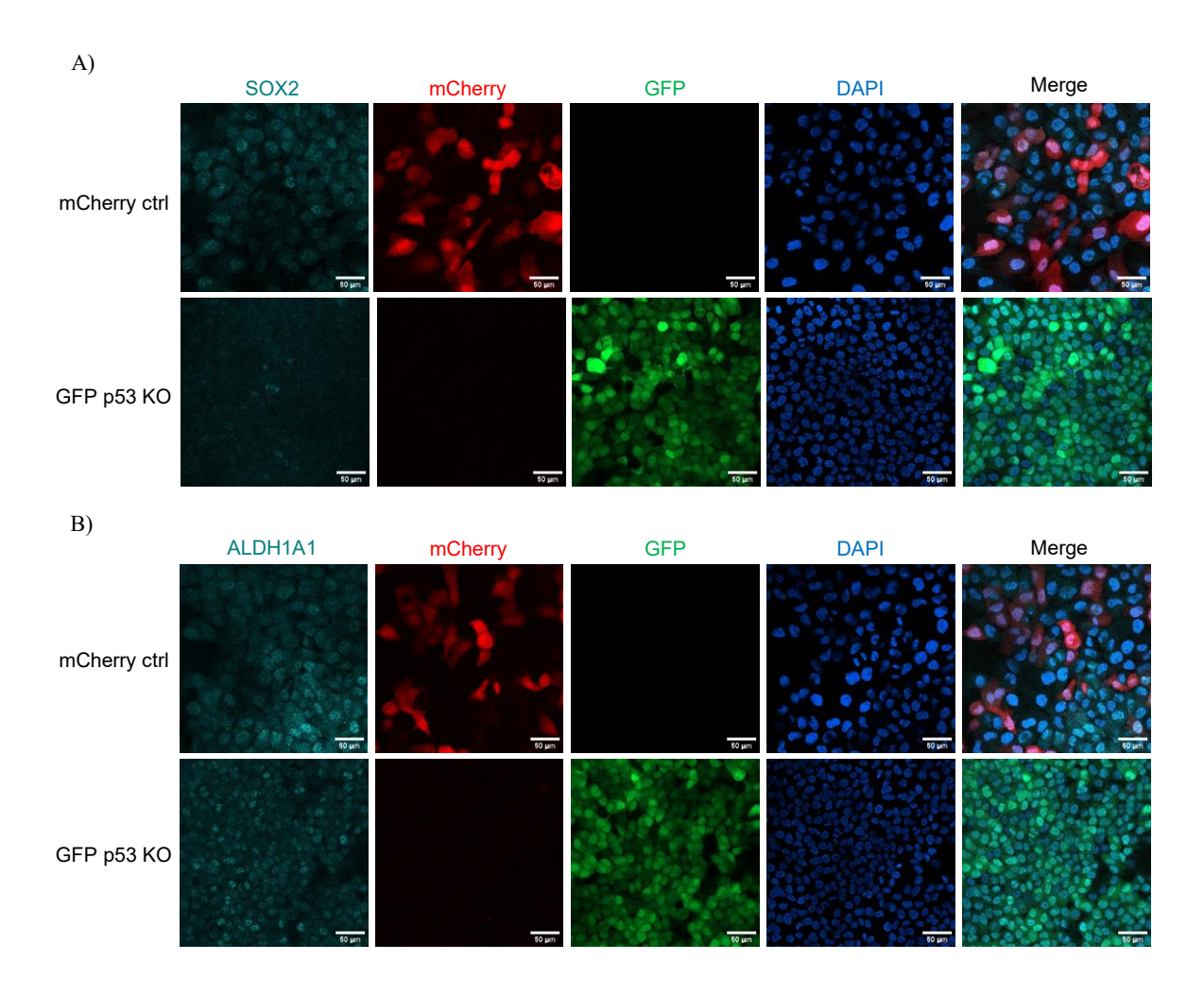


Figure: 12 Expression of cancer stemness markers in mutp53 versus p53 KO cells.

Representative confocal images showing SOX2 (A) and ALDH1A1 (B) expression in A431 mCherry control versus GFP KO cells. Fluorescent cells were stained with rabbit anti-SOX2 or anti-ALDH1A1 (1:100) and Alexa Fluor 647-conjugated donkey anti-rabbit (1:250) antibodies. Scale bar = $50\mu m$.

5.2.2. Engulfing cells express cancer stemness markers

Having shown that mutp53 cells express SOX2 and ALDH1A1, we went on to examine the localisation of these markers in CIC structures compared with surrounding cells. Mutp53 and KO CIC co-cultures were established and fixed after 24 hours for immunofluorescence staining. Again, a secondary antibody-only negative control was used, and the same settings were applied to all images.

The confocal data showed ALDH1A1 to be concentrated within engulfing cells, supporting our hypothesis that this subpopulation corresponds to the CSCs (Figure 14). SOX2 on the other hand was more localised to internal cells, and unexpectedly, outside of its normal location in the nucleus (Figure 13). Despite different subcellular locations, both markers were clearly upregulated in CIC structures versus surrounding cells, suggesting a clear association between cell engulfment and cancer stemness.

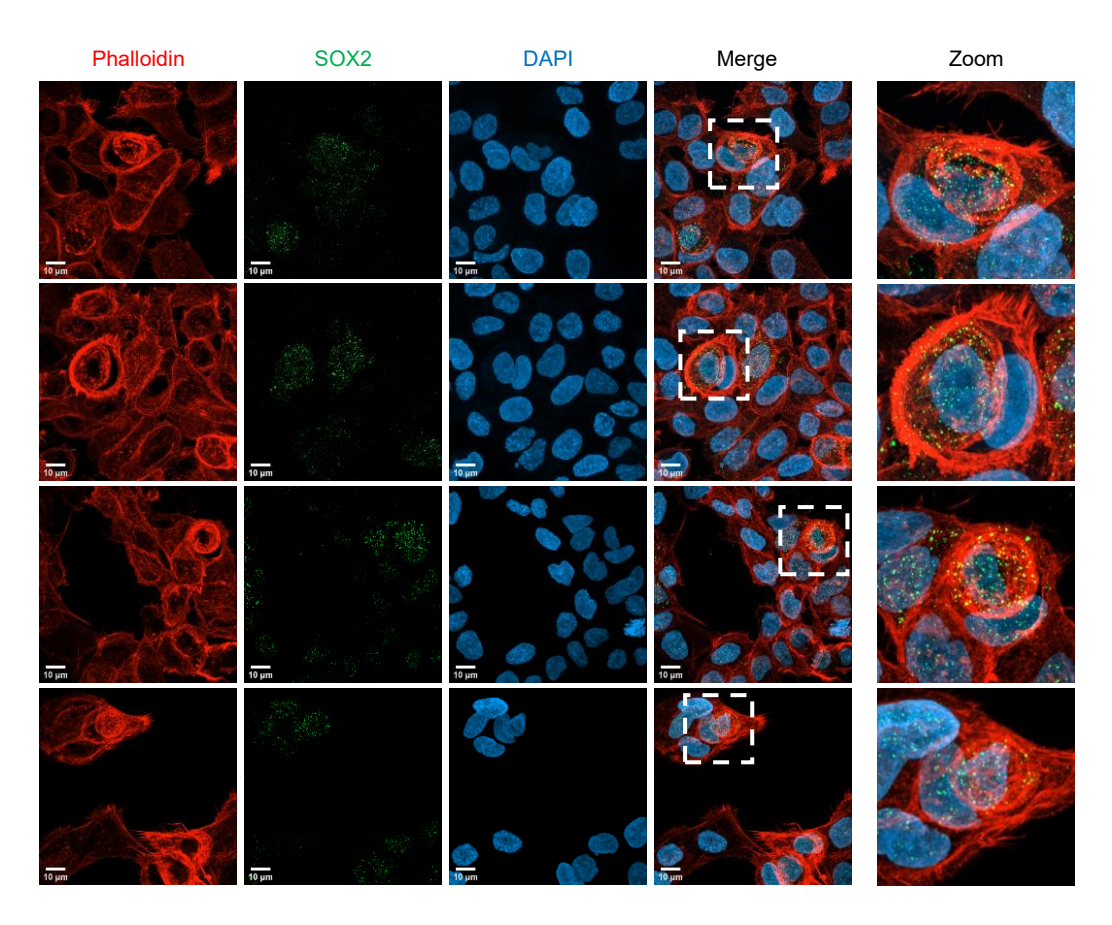


Figure 13: SOX2 expression is concentrated in CIC structures.

Confocal Z-projections of CIC structures from A431 control/KO co-cultures. Cells were stained with rabbit anti-SOX2 (1:100) and Alexa Fluor 488-conjugated donkey anti-rabbit (1:250) antibodies, then labelled with phalloidin and DAPI. Zoomed images show SOX2 concentrated in internalised cells, appearing to leave the nucleus. Scale $bar = 10 \mu m.$

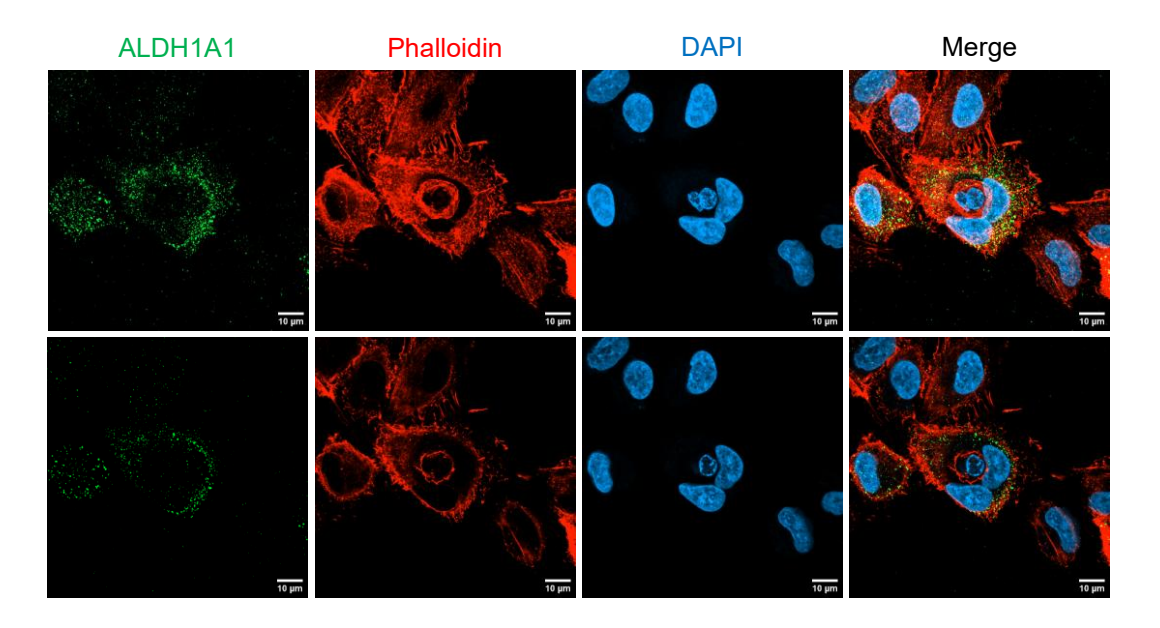


Figure 14: Engulfing cells express ALDH1A1.

Confocal imaging of ALDH1A1 expression in CIC structures. Non-fluorescent A431 cells were stained with rabbit anti-ALDH1A1 (1:100) and Alexa Fluor 488-conjugated donkey anti-rabbit (1:250) antibodies. *Above:* Maximum intensity Z-projection showing a multinucleated host cell expressing ALDH1A1 (green). *Below:* Representative slice showing ALDH1A1 expression concentrated around the edge of the engulfing cell. Scale bar = 10µm.

5.3. Discussion

Numerous studies have cited cancer stemness as a GOF effect of mutp53, as evidenced through expression of CSC markers. Notably, in colorectal cancer, mutp53 promotes the expression of ALDH1A1 (Solomon et al., 2018). Similarly, mesenchymal stem cell (MSC) tumours harbouring GOF p53 mutations show enhanced expression of SOX2 (Koifman et al., 2018). Corroborating this, we saw clear expression of ALDH1A1 and SOX2 in mutp53 A431 cells using immunofluorescence (Figure 12).

Cancer stemness has also been associated with CIC formation; for example, aggressive breast cancer cells have been shown to engulf MSCs (Chen et al., 2019). This benefits the engulfing cancer cells as they acquire stem-like traits (evidenced through SOX2 upregulation), as well as increased invasiveness and metastatic potential. Mechanistically, the authors speculated that CIC formation facilitates cell fusion and gene transfer from the internal to host cell, thereby promoting host cell tumorgenicity.

In our confocal data, SOX2 and ALDH1A1 were concentrated within CIC structures relative to surrounding cells. SOX2 was particularly prevalent in internal cells, notably residing in the cytoplasm rather than its normal location in the nucleus (Figure 13). Perhaps this reflects an intermediate stage in the transfer of SOX2 from internal to engulfing cells at time of fixation.

Together, these findings reveal a clear upregulation of SOX2 and ALDH1A1 in CIC structures, suggesting an association between cell engulfment and cancer stemness. However, further work will be needed to better understand the specific localisation of these markers within CIC structures, and how this relates to the mechanisms and consequences of engulfment. Building on the observations of Chen et al., it could be worthwhile to co-culture mutp53 cells with MSCs and explore through immunofluorescence whether the resultant CIC structures convey stem-like traits to mutp53 hosts. Further work investigating a wider array of cancer stemness markers may also provide further insights, for instance, CD44 and Lgr5 which have both been associated with GOF mutp53 (Solomon et al., 2018).

Chapter 6: Conclusions and future directions

6.1. Key conclusions

The overarching aim of this project was to investigate the mechanisms of cell engulfment by mutp53 cancer cells. This involved examining the role of SH3BGRL in driving engulfment and promoting mutp53's GOF activity, as well as investigating a potential link between CIC formation and cancer stemness. The main conclusions are that:

- the mechanisms of mutp53-driven engulfment are reminiscent of cell cannibalism rather than entosis.
- mutp53-dependent engulfment is driven by expression of SH3BGRL (Dolma et al., 2025).
- SH3BGRL expression promotes anchorage-independent growth, a GOF phenotype of mutp53.
- CIC structures exhibit enhanced expression of the cancer stemness markers SOX2 and ALDH1A1 compared with surrounding cells.

6.2. Future directions

One of our hypotheses was that the determination of host versus internal cell fate depends on differences in membrane tension between the two neighbouring cells. To investigate this, we used FLIM with the Flipper-TR tension-sensing probe to compare membrane tension between mutp53 and p53 KO cultures, as well as within CIC structures. Future experiment ideas include examining plasma membrane tension in control and KO cells overexpressing RhoA, given its importance in driving entosis (Sun et al., 2014). It could also be interesting to compare tensions before and after inducing mutp53 expression with doxycycline.

Another experimental approach that could provide valuable insight into the mechanisms of CIC formation is a dual optical trap. This would involve bringing two cells together and releasing one or the other to determine which drives CIC formation. Mutp53 and KO cells could be brought together, as well as cells with and without RhoA overexpression.

It is also important to appreciate that the mechanisms of CIC formation *in vitro* may not accurately reflect those occurring in patients. Further work with *in vivo* tumour models, for example, mouse xenografts, will therefore be important in elucidating the physiological relevance of this process and its impacts on tumour progression.

Given the technical challenges we encountered assessing anchorage-independent growth via colony formation assays, an *in vivo* metastasis model could offer a more effective means of evaluating the impacts of CIC formation long-term. CIC-rich co-cultures of mutp53 and KO cells could be xenografted into mice, alongside control injections of mutp53 cells alone. The rates of metastasis could then be compared between the two conditions; for example, using an *in vivo* imaging system, given that the cells are already endogenously fluorescent. Mackay et al. (2018) previously showed that CIC-enriched mutp53 xenografts increase tumour size; however, metastatic potential has not yet been investigated. Therefore, if successful, this experiment could provide valuable insight into the potential of CIC formation to enhance anchorage-independent survival and tumour dissemination.

6.3. Wider significance

Research into CIC in cancer has potential translational applications. Our lab has shown that mutp53 cells exhibit enhanced ability to engulf large beads compared to p53 KO cells (Dolma et al., 2025). Excitingly, they can also take up 'drug-loaded vesicles', designed to mimic the composition of the plasma membrane and filled with chemotherapies such as doxorubicin. This suggests a promising avenue for selectively targeting the engulfing cells.

This approach becomes particularly interesting when considering the possibility of the engulfing cell population as the cancer stem cells. Given their importance in driving tumour initiation and resistance to therapy (Zhao et al., 2017), a novel CSC-specific drug delivery route could be very valuable.

Beyond its therapeutic promise, continued investigation into cell engulfment in cancer remains essential. The molecular mechanisms driving CIC formation are still poorly defined and may vary substantially across tumour types and p53 expression states. Dissecting these pathways could provide valuable insight into the impacts of CIC formation on tumour progression, and explain why this process is frequently associated with aggressive disease phenotypes and poor patient outcomes.

Bibliography

Abdullah, L. N. and Chow, E. K.-H. (2013) 'Mechanisms of chemoresistance in cancer stem cells.' *Clinical and Translational Medicine*, 2(1) 3.

Al-Hajj, M., Wicha, M. S., Benito-Hernandez, A., Morrison, S. J. and Clarke, M. F. (2003) 'Prospective identification of tumorigenic breast cancer cells.' *Proceedings of the National Academy of Sciences*, 100(7) 3983–3988.

Alvarado-Ortiz, E., de la Cruz-López, K. G., Becerril-Rico, J., Sarabia-Sánchez, M. A., Ortiz-Sánchez, E. and García-Carrancá, A. (2021) 'Mutant p53 Gain-of-Function: Role in Cancer Development, Progression, and Therapeutic Approaches.' *Frontiers in Cell and Developmental Biology*, 8, Article 607670.

Belostotskaya, G. B., Nerubatskaya, I. V. and Galagudza, M. M. (2018) 'Two mechanisms of cardiac stem cell-mediated cardiomyogenesis in the adult mammalian heart include formation of colonies and cell-in-cell structures.' *Oncotarget*, 9(75) 34159–34175.

Bocci, F., Levine, H., Onuchic, J. N. and Jolly, M. K. (2019) 'Deciphering the Dynamics of Epithelial-Mesenchymal Transition and Cancer Stem Cells in Tumor Progression.' *Current Stem Cell Reports*, 5(1) 11–21.

Bonnet, D. and Dick, J. E. (1997) 'Human acute myeloid leukemia is organized as a hierarchy that originates from a primitive hematopoietic cell.' *Nature Medicine*, 3(7) 730–737.

Bozkurt, E., Düssmann, H., Salvucci, M., Cavanagh, B. L., Van Schaeybroeck, S., Longley, D. B., Martin, S. J. and Prehn, J. H. M. (2021) 'TRAIL signaling promotes entosis in colorectal cancer.' *Journal of Cell Biology*, 220(11) e202010030.

Cabrera, M. C., Hollingsworth, R. E. and Hurt, E. M. (2015) 'Cancer stem cell plasticity and tumor hierarchy.' *World Journal of Stem Cells*, 7(1) 27–36.

Cano, C. E., Sandí, M. J., Hamidi, T., Calvo, E. L., Turrini, O., Bartholin, L., Loncle, C., Secq, V., Garcia, S., Lomberk, G., Kroemer, G., Urrutia, R. and Iovanna, J. L. (2012) 'Homotypic cell cannibalism, a cell-death process regulated by the nuclear protein 1, opposes to metastasis in pancreatic cancer.' *EMBO Molecular Medicine*, 4(9) 964–979.

Chen, Y.-C., Gonzalez, M. E., Burman, B., Zhao, X., Anwar, T., Tran, M., Medhora, N., Hiziroglu, A. B., Lee, W., Cheng, Y.-H., Choi, Y., Yoon, E. and Kleer, C. G. (2019) 'Mesenchymal Stem/Stromal Cell Engulfment Reveals Metastatic Advantage in Breast Cancer.' *Cell Reports*, 27(13) 3916-3926, e5.

Dolma, L., Patterson, M. I., Banyard, A., Hall, C., Bell, S., Breitwieser, W., Sahoo, S., Weightman, J., Gil, M. P., Ashton, G., Behan, C., Fullard, N., Williams, L. D. and Muller, P. A. (2025) 'Mutant p53 induces SH3BGRL expression to promote cell engulfment.' *Cell Death Discovery*, 11(1) 288.

Dong, P., Karaayvaz, M., Jia, N., Kaneuchi, M., Hamada, J., Watari, H., Sudo, S., Ju, J. and Sakuragi, N. (2013) 'Mutant p53 gain-of-function induces epithelial-mesenchymal transition through modulation of the miR-130b–ZEB1 axis.' *Oncogene*, 32(27) 3286–3295.

Druzhkova, I., Potapov, A., Ignatova, N., Bugrova, M., Shchechkin, I., Lukina, M., Shimolina, L., Kolesnikova, E., Shirmanova, M. and Zagaynova, E. (2024) 'Cell hiding in colorectal cancer: correlation with response to chemotherapy in vitro and in vivo.' *Scientific Reports*, 14(1) 28762.

Du, F., Zhao, X. and Fan, D. (2017) 'Soft Agar Colony Formation Assay as a Hallmark of Carcinogenesis.' *Bio-protocol*, 7(12) e2351.

Durgan, J., Tseng, Y.-Y., Hamann, J. C., Domart, M.-C., Collinson, L., Hall, A., Overholtzer, M. and Florey, O. (2017) 'Mitosis can drive cell cannibalism through entosis.' *eLife*, e27134. Eberth, J. (1864) 'Über die feineren bau der darmschleithaut.' *Wurzb Naturwiss Zeitschr*, 5(11).

Egeo, A., Mazzocco, M., Arrigo, P., Vidal-Taboada, J. M., Oliva, R., Pirola, B., Giglio, S., Rasore-Quartino, A. and Scartezzini, P. (1998) 'Identification and Characterization of a New Human Gene Encoding a Small Protein with High Homology to the Proline-Rich Region of the SH3BGR Gene.' *Biochemical and Biophysical Research Communications*, 247(2) 302–306.

Fais, S. and Overholtzer, M. (2018) 'Cell-in-cell phenomena, cannibalism, and autophagy: is there a relationship?' *Cell Death & Disease*, 9(2) 1–3.

Feroz, W. and Sheikh, A. M. A. (2020) 'Exploring the multiple roles of guardian of the genome: P53.' *Egyptian Journal of Medical Human Genetics*, 21(1) 49.

Ghatak, D., Datta, A., Roychowdhury, T., Chattopadhyay, S. and Roychoudhury, S. (2021) 'MicroRNA-324-5p–CUEDC2 Axis Mediates Gain-of-Function Mutant p53-Driven Cancer Stemness.' *Molecular Cancer Research*, 19(10) 1635–1650.

Gibbs, C. P., Kukekov, V. G., Reith, J. D., Tchigrinova, O., Suslov, O. N., Scott, E. W., Ghivizzani, S. C., Ignatova, T. N. and Steindler, D. A. (2005) 'Stem-Like Cells in Bone Sarcomas: Implications for Tumorigenesis.' *Neoplasia*, 7(11) 967–976.

Guadamillas, M. C., Cerezo, A. and del Pozo, M. A. (2011) 'Overcoming anoikis – pathways to anchorage-independent growth in cancer.' *Journal of Cell Science*, 124(19) 3189–3197. Hamann, J. C., Surcel, A., Chen, R., Teragawa, C., Albeck, J. G., Robinson, D. N. and Overholtzer, M. (2017) 'Entosis Is Induced by Glucose Starvation.' *Cell Reports*, 20(1) 201–210. Hanahan, D. and Weinberg, R. A. (2011) 'Hallmarks of Cancer: The Next Generation.' *Cell*, 144(5) 646–674.

- Jaumouillé, V. and Waterman, C. M. (2020) 'Physical Constraints and Forces Involved in Phagocytosis.' *Frontiers in Immunology*, 11, Article 1097.
- Koifman, G., Shetzer, Y., Eizenberger, S., Solomon, H., Rotkopf, R., Molchadsky, A., Lonetto, G., Goldfinger, N. and Rotter, V. (2018) 'A Mutant p53-Dependent Embryonic Stem Cell Gene Signature Is Associated with Augmented Tumorigenesis of Stem Cells.' *Cancer Research*, 78(20) 5833–5847.
- Krajcovic, M., Johnson, N. B., Sun, Q., Normand, G., Hoover, N., Yao, E., Richardson, A. L., King, R. W., Cibas, E. S., Schnitt, S. J., Brugge, J. S. and Overholtzer, M. (2011) 'A non-genetic route to aneuploidy in human cancers.' *Nature Cell Biology*, 13(3) 324–330.
- Lang, G. A., Iwakuma, T., Suh, Y.-A., Liu, G., Rao, V. A., Parant, J. M., Valentin-Vega, Y. A., Terzian, T., Caldwell, L. C., Strong, L. C., El-Naggar, A. K. and Lozano, G. (2004) 'Gain of Function of a p53 Hot Spot Mutation in a Mouse Model of Li-Fraumeni Syndrome.' *Cell*, 119(6) 861–872.
- Lei, M. M. L. and Lee, T. K. W. (2021) 'Cancer Stem Cells: Emerging Key Players in Immune Evasion of Cancers.' *Frontiers in Cell and Developmental Biology*, 9, Article 692940.
- Li, C., Heidt, D. G., Dalerba, P., Burant, C. F., Zhang, L., Adsay, V., Wicha, M., Clarke, M. F. and Simeone, D. M. (2007) 'Identification of Pancreatic Cancer Stem Cells.' *Cancer Research*, 67(3) 1030–1037.
- Li, H., Zhang, M., Wei, Y., Haider, F., Lin, Y., Guan, W., Liu, Y., Zhang, S., Yuan, R., Yang, X., Yang, S. and Wang, H. (2020) 'SH3BGRL confers innate drug resistance in breast cancer by stabilizing HER2 activation on cell membrane.' *Journal of Experimental & Clinical Cancer Research*, 39(1) 81.
- Li, Y., Sun, X. and Dey, S. K. (2015) 'Entosis Allows Timely Elimination of the Luminal Epithelial Barrier for Embryo Implantation.' *Cell Reports*, 11(3) 358–365.
- Liang, Y., Zhong, Z., Huang, Y., Deng, W., Cao, J., Tsao, G., Liu, Q., Pei, D., Kang, T. and Zeng, Y.-X. (2010) 'Stem-like Cancer Cells Are Inducible by Increasing Genomic Instability in Cancer Cells.' *Journal of Biological Chemistry*. Elsevier, 285(7) 4931–4940.
- Liu, Z., Xu, W., Tan, X. and Li, C. (2021) 'EZH2-mediated epigenetic suppression of SH3BGRL potently inhibits lung cancer progression.' *Biochemical and Biophysical Research Communications*, 548, April, 53–59.
- Lugini, L., Matarrese, P., Tinari, A., Lozupone, F., Federici, C., Iessi, E., Gentile, M., Luciani, F., Parmiani, G., Rivoltini, L., Malorni, W. and Fais, S. (2006) 'Cannibalism of Live Lymphocytes by Human Metastatic but Not Primary Melanoma Cells.' *Cancer Research*, 66(7) 3629–3638.
- Mackay, H. L., Moore, D., Hall, C., Birkbak, N. J., Jamal-Hanjani, M., Karim, S. A., Phatak, V. M., Piñon, L., Morton, J. P., Swanton, C., Le Quesne, J. and Muller, P. A. J. (2018) 'Genomic instability in mutant p53 cancer cells upon entotic engulfment.' *Nature Communications*, 9(1) 3070.

Mackay, H. L. and Muller, P. A. J. (2019) 'Biological relevance of cell-in-cell in cancers.' *Biochemical Society Transactions*, 47(2) 725–732.

Millarte, V. and Farhan, H. (2012) 'The Golgi in Cell Migration: Regulation by Signal Transduction and Its Implications for Cancer Cell Metastasis.' *The Scientific World Journal*, 498278.

Moll, U. M. and Petrenko, O. (2003) 'The MDM2-p53 Interaction.' *Molecular Cancer Research*, 1(14) 1001–1008.

Muller, P. A. J., Caswell, P. T., Doyle, B., Iwanicki, M. P., Tan, E. H., Karim, S., Lukashchuk, N., Gillespie, D. A., Ludwig, R. L., Gosselin, P., Cromer, A., Brugge, J. S., Sansom, O. J., Norman, J. C. and Vousden, K. H. (2009) 'Mutant p53 Drives Invasion by Promoting Integrin Recycling.' *Cell*, 139(7) 1327–1341.

Muller, P. A. J. and Vousden, K. H. (2013) 'p53 mutations in cancer.' Nature Cell Biology, 15(1) 2–8.

Olive, K. P., Tuveson, D. A., Ruhe, Z. C., Yin, B., Willis, N. A., Bronson, R. T., Crowley, D. and Jacks, T. (2004) 'Mutant *p53* Gain of Function in Two Mouse Models of Li-Fraumeni Syndrome.' *Cell*, 119(6) 847–860.

Overholtzer, M. and Brugge, J. S. (2008) 'The cell biology of cell-in-cell structures.' *Nature Reviews Molecular Cell Biology*, 9(10) 796–809.

Overholtzer, M., Mailleux, A. A., Mouneimne, G., Normand, G., Schnitt, S. J., King, R. W., Cibas, E. S. and Brugge, J. S. (2007) 'A Nonapoptotic Cell Death Process, Entosis, that Occurs by Cell-in-Cell Invasion.' *Cell*, 131(5) 966–979.

Park, E. K., Lee, J. C., Park, J. W., Bang, S. Y., Yi, S. A., Kim, B. K., Park, J. H., Kwon, S. H., You, J. S., Nam, S. W., Cho, E. J. and Han, J. W. (2015) 'Transcriptional repression of cancer stem cell marker CD133 by tumor suppressor p53.' *Cell Death & Disease*. Nature Publishing Group, 6(11) e1964–e1964.

Ricci-Vitiani, L., Lombardi, D. G., Pilozzi, E., Biffoni, M., Todaro, M., Peschle, C. and De Maria, R. (2007) 'Identification and expansion of human colon-cancer-initiating cells.' *Nature*, 445(7123) 111–115.

Rich, J. N. (2016) 'Cancer stem cells: understanding tumor hierarchy and heterogeneity.' *Medicine*, 95(1S) S2.

Roffay, C., García-Arcos, J. M., Chapuis, P., López-Andarias, J., Schneider, F., Colom, A., Tomba, C., Meglio, I. D., Dunsig, V., Matile, S., Roux, A. and Mercier, V. (2023) 'Technical insights into fluorescence lifetime microscopy of mechanosensitive Flipper probes.' *bioRxiv* [preprint: accessed 17.7.25].

- Saleh, A. A. M., Haider, F., Lv, H., Liu, B., Xiao, J., Zhang, M., Zheng, Y., Yang, S. and Wang, H. (2023) 'SH3BGRL Suppresses Liver Tumor Progression through Enhanced ATG5-Dependent Autophagy.' *Journal of Oncology*, 2023(1) 1105042.
- Sarig, R., Rivlin, N., Brosh, R., Bornstein, C., Kamer, I., Ezra, O., Molchadsky, A., Goldfinger, N., Brenner, O. and Rotter, V. (2010) 'Mutant p53 facilitates somatic cell reprogramming and augments the malignant potential of reprogrammed cells.' *The Journal of Experimental Medicine*, 207(10) 2127–2140.
- Shiozawa, Y., Nie, B., Pienta, K. J., Morgan, T. M. and Taichman, R. S. (2013) 'Cancer stem cells and their role in metastasis.' *Pharmacology & Therapeutics*, 138(2) 285–293.
- Solomon, H., Dinowitz, N., Pateras, I. S., Cooks, T., Shetzer, Y., Molchadsky, A., Charni, M., Rabani, S., Koifman, G., Tarcic, O., Porat, Z., Kogan-Sakin, I., Goldfinger, N., Oren, M., Harris, C. C., Gorgoulis, V. G. and Rotter, V. (2018) 'Mutant p53 gain of function underlies high expression levels of colorectal cancer stem cells markers.' *Oncogene*, 37(12) 1669–1684.
- Soussi, T. and Wiman, K. G. (2015) 'TP53: an oncogene in disguise.' *Cell Death and Differentiation*, 22(8) 1239.
- Sun, Q., Huang, H. and Overholtzer, M. (2015) 'Cell-in-cell structures are involved in the competition between cells in human tumors.' *Molecular & Cellular Oncology*, 2(4) e1002707.
- Sun, Q., Luo, T., Ren, Y., Florey, O., Shirasawa, S., Sasazuki, T., Robinson, D. N. and Overholtzer, M. (2014) 'Competition between human cells by entosis.' *Cell Research*, 24(11) 1299–1310. Sun, Q. and Overholtzer, M. (2013) 'Methods for the Study of Entosis.' *In* McCall, K. and Klein, C. (eds) *Necrosis: Methods and Protocols*. Totowa, NJ: Humana Press, 59–66.
- Wang, H., Liu, B., Al-Aidaroos, A. Q. O., Shi, H., Li, L., Guo, K., Li, J., Tan, B. C. P., Loo, J. M., Tang, J. P., Thura, M. and Zeng, Q. (2016) 'Dual-faced SH3BGRL: oncogenic in mice, tumor suppressive in humans.' *Oncogene*, 35(25) 3303–3313.
- Wang, S., He, M., Li, L., Liang, Z., Zou, Z. and Tao, A. (2016) 'Cell-in-Cell Death Is Not Restricted by Caspase-3 Deficiency in MCF-7 Cells.' *Journal of Breast Cancer*, 19(3) 231–241.
- Xu, L., Zhang, M., Li, H., Guan, W., Liu, B., Liu, F., Wang, Hehua, Li, J., Yang, S., Tong, X. and Wang, Haihe (2018) 'SH3BGRL as a novel prognostic biomarker is down-regulated in acute myeloid leukemia.' *Leukemia & Lymphoma*, 59(4) 918–930.
- Yang, X., Wang, Y., Rong, S., An, J., Lan, X., Yin, B., Sun, Y., Wang, P., Tan, B., Xuan, Y., Xie, S., Su, Z. and Li, Y. (2023) 'Gene SH3BGRL3 regulates acute myeloid leukemia progression through circRNA_0010984 based on competitive endogenous RNA mechanism.' *Frontiers in Cell and Developmental Biology*, Volume 11.

Yin, L., Xiang, Y., Zhu, D.-Y., Yan, N., Huang, R.-H., Zhang, Y. and Wang, D.-C. (2005) 'Crystal structure of human SH3BGRL protein: The first structure of the human SH3BGR family representing a novel class of thioredoxin fold proteins.' *Proteins: Structure, Function, and Bioinformatics*, 61(1) 213–216.

Yue, X., Zhao, Y., Xu, Y., Zheng, M., Feng, Z. and Hu, W. (2017) 'Mutant p53 in Cancer: Accumulation, Gain-of-Function, and Therapy.' *Journal of Molecular Biology*, 429(11) 1595–1606.

Zhao, W., Li, Y. and Zhang, X. (2017) 'Stemness-Related Markers in Cancer.' *Cancer translational medicine*, 3(3) 87–95.

Zhao, Y., Li, Y., Sheng, J., Wu, F., Li, K., Huang, R., Wang, X., Jiao, T., Guan, X., Lu, Y., Chen, X., Luo, Z., Zhou, Y., Hu, H., Liu, W., Du, B., Miao, S., Cai, J., Wang, L., Zhao, H., Ying, J., Bi, X. and Song, W. (2019) 'P53-R273H mutation enhances colorectal cancer stemness through regulating specific lncRNAs.' *Journal of Experimental & Clinical Cancer Research*, 38, 379.